Dominik Bulfon, BSc

Basic Insights into BMP Synthesis and its Role in Drug-Induced Phospholipidosis

MASTER'S THESIS

to achieve the university degree of

Master of Science

Master's degree programme: Biochemistry and Molecular Biomedical Sciences

submitted to

Graz University of Technology

Supervisor

Assoc. Univ.-Prof. Mag. Dr.rer.nat. Robert Zimmermann

Institute of Moleculare Biosciences
Heinrichstrasse 31/II, 8010 Graz, Austria

Graz, March 2019

AFFIDAVIT

I declare that I have authored this thesis independently, that I have not used other than the declared sources/resources, and that I have explicitly indicated all material which has been quoted either literally or by content from the sources used. The text document uploaded to TUGRAZonline is identical to the present master‘s thesis.

Date

Signature

Index

Acknowledgment

Firstly, I want to thank my supervisor Prof. Dr. Robert Zimmermann for having me as his master student and. I am very grateful for his continuous support and help for me to become a better scientist. I also want to thank Gernot Grabner and Nermeen Girgis for teaching me new methods and providing answers to all the questions that I had. Another big thank you goes out to all my other colleagues and members of the institute, who created an enjoyable working atmosphere.

But the biggest thank you goes out to my parents, as they supported (not only financially) me before, currently, and after all of my studies.

Abstract

Bis(monoacylglycero)phosphate (BMP) is a negatively charged, low abundant phospholipid, mainly encountered in late endosomes and lysosomes. BMP features a unique *sn*-1: *sn*-1' stereoconfiguration and is highly increased in genetic and drug-induced lysosomal storage disorders (LSD). BMP has an important role in endosomal /lysosomal maturation, as well as lipid degradation and sorting. Nevertheless, the molecular pathways of BMP synthesis are unknown.

In this thesis, we investigated basic mechanisms of BMP synthesis and its role in drug-induced LSD. We show that phosphatidylglycerol (PG) 18:1 acts as a precursor of BMP in various cell lines and that BMP is rather formed in the cytoplasm than in acidic organelles. Furthermore, we provide evidence that it can be synthesized in the extracellular compartments by enzymes secreted from macrophages. By inhibition of phospholipase D1 (PLD1) and acyl-CoA synthetase (ACS), we observed significant decrease in intracellular BMP biosynthesis. These observations indicate that PLD1 activity and acyl-CoAs are required for efficient BMP formation.

To examine the implication of BMP in drug-induced LSD, we investigated whether increased BMP synthesis in COS7 cells affects the survivability when treated with the cationic amphiphilic drug (CAD) amiodarone. CADs are drugs that can cause LSD by interacting with phospholipids or lysosomal enzymes mediating their degradation. This can lead to severe cell damage and cell death. BMP enriched cells treated with amiodarone showed a significant increased viability suggesting that BMP has protective function.

In summary, our study provides novel insights into BMP biosynthesis and indicates that cellular BMP accumulation protects from CAD-induced cytotoxicity.

Zusammenfassung

Bis(monoacylglycero)phosphat (BMP) ist ein negatives geladenes, selten vorkommendes Phospholipid, das hauptsächlich in späten Endosomen und Lysosomen vorzufinden ist. BMP zeigt eine einzigartige *sn*-1: *sn*-1‘ Stereokonfiguration und ist bei genetischen und Medikamenten-induzierten lysosomalen Speicherkrankheiten (LSD) stark angereichert. BMP spielt sowohl in der lysosomalen/endosomalen Biogenese, als auch im Abbau und in der Sortierung von Lipiden eine wichtige Rolle, dennoch sind die molekularen Mechanismen der BMP Synthese unbekannt.

In dieser Arbeit untersuchten wir grundlegende Mechanismen der BMP Synthese und dessen Rolle in Medikamenten-induzierten LSDs. Wir zeigen, dass Phosphatidylglycerol (PG) 18:1 in mehreren Zelllinien als Vorstufe von BMP agiert und dass BMP eher im Zytoplasma, als in sauren Organellen synthetisiert wird. Des Weiteren konnten wir eine extrazelluläre BMP Formierung durch sekretierte Enzyme von Makrophagen nachweisen. Durch die Inhibierung von Phospholipase D1 (PLD1) und Acyl-CoA-Synthetase (ACS), beobachteten wir eine starke Reduzierung der intrazellulären BMP Biosynthese, was auf eine Beteiligung von PLD1 Aktivität und Acyl-CoAs in der BMP Synthese hindeutet.

Um die Rolle von BMP in Medikamenten-induzierten LSDs zu ermitteln, untersuchten wir ob erhöhte BMP Synthese das Überleben von COS7 Zellen beeinflusst, die mit dem kationisch-amphiphilen Medikament (CAD) Amiodaron behandelt wurden. CADs sind Medikamente welche LSDs hervorrufen können, indem sie mit Phospholipiden oder mit lysosomalen Enzymen interagieren. Dies kann zu ernster zellulärer Schädigung und Zelltod führen. Mit BMP angereicherte Zellen zeigten eine signifikant erhöhte Lebensfähigkeit, was darauf hinweist, dass BMP eine protektive Funktion besitzt.

Zusammenfassend geben unsere Untersuchungen neue Einsichten in die BMP Synthese und lassen vermuten, dass eine zelluläre BMP Anreicherung vor CAD-induzierter Zytotoxizität schützt.

Abbreviations

Alix	Apoptosis-linked interacting protein X
ADP	Adenosine diphosphate
Akt	Protein Kinase B
ARF	ADP-ribosylation factor
ASM	Acid sphingomyelinase
BDP	Bis(diacylglycero)phosphate
BMP	Bis(monoacylglycero)phosphate
BSA	Bovine Serum Albumin
CAD	Cationic amphiphilic drugs
Cer	Ceramide
DG	Diacylglycerol
DMEM	Dulbecco's modified eagle medium
EDTA	Ethylendiamintetraacetic acid
EE	Early endosome
ER	Endoplasmatic reticulum
ESCRT	Endosomal sorting complex required for transport
EtBr	Ethidiumbromid
FA	Fatty acid
GPG	Glycerophosphoglycero
Hemi-BDP	Hemi-Bis(diacylglycero)phosphate
ILV	Intraluminal vesicles
LBPA	Lysobisphosphatidic acid
LDH	Lactate dehydrogenase
LE	Late endosome
LPA	Lysophosphatidic acid
LPC	Lysophosphatidylcholine
LPG	Lysophosphatidylglycerol
LSD	Lysosomal storage disorder
MG	Monoacylglycerol
MVB	Multivesicular bodies
OMV	Outermembrane vesicle

PAGE	Polyacrlyamid gelelectrophoresis
PA	Phosphatidic acid
PC	Phosphatidylcholine
PCR	Polymerase chain reaction
PE	Phosphatidylethanolamine
PG	Phosphatidylglycerol
PL	Phospholipid
PLA	Phospholipase A
PLD	Phospholipase D
PUFA	Polyunsaturated fatty acid
SAP	Sphingolipid activator protein
SDS	Sodiumdodecylsulfate
SL	Sphingolipid
TG	Triacylglycerol

1. Introduction

1.1. BMP Structure and Function

Bis(monoacylglycero)phosphate (BMP) was discovered in 1967 by Body and Gray[1] isolated from pig and rabbit lung. It is a negatively charged phospholipid, which features a unique *sn*-1: *sn*-1′ stereo configuration[2] (Figure 1). BMP is also commonly referred as “funny” lipid, or lyso-bis-phosphatidic acid (LBPA). However, the term LBPA is misleading as the “bis” prefix implies that there are two phosphatidic acids linked together, with one or two fatty acid residues in positions 2 and 3 of the glycerol moities[3]. BMP is present in most mammalian cells and tissues, where it is a low abundant lipid accounting for 1-2% of the total phospholipids. It is highly enriched (up to 18% of total phospholipids) in lysosomes and late endosomes[4]. BMP represents a family of compounds with a glycerophosphoglycerol (GPG) backbone which differ in length and saturation of their acyl chains. Oleic acid was found to be the most prominent acyl chain with up to 50-80% in BHK cells[5], alveolar macrophages[6], and rat liver[7]. Polyunsaturated fatty acids (PUFA) in BMP like arachidonic acid and docosahexaenoic acid (22:6n-3) are found in human liver, rat, and THP-1 RAW macrophages[7–10]. This variation in the fatty acid composition of BMP is considered to affect its biochemical function. BMP containing PUFA does not tightly pack within membrane structures, thus favoring membrane fusion and membrane fluidity.

BMP is compartmentalized in inner endosomal membrane domains. Endosomes display multiple roles by staging endocytosed materials which either undergoe recycling back to the plasma membrane (early and recycling endosomes), cellular distribution by specialized organelles (LE/lysosomes), or degradation[2,11] (Figure 2). Lysosomes are the final destination for degradative products, whereas the LE is considered to be a sorting and dynamic organelle, with transporting function[2,11]. Large structures called multi vesicular bodies (MVB) transport intermediates along the degradation pathway. The MVBs move towards the LE and fuse. Luzio and Pryor[12] claim, that LE and lysosomes form hybrid organelles by constant fusion and fission. LE and lysosomes are both fusogenic and share similar characteristics, which

makes them hard to distinguish. However, each organelle possesses a characteristic lipid and protein composition making endosome maturation traceable. It has been shown that BMP plays an important role in the regulation and dynamics of internal membranes inside these organelles[13]. Due to the *sn*-1: *sn*-1' configuration, BMP is predicted to have a cone-shaped structure, which may induces invagination and membrane asymmetry in BMP-rich domains. This prediction is underlined by Matuso et al.[13], who reported intrinsic ability of BMP to form such multivesicular structures. A keyplayer of multivesicular liposome formation is a cytosolic protein associated to ESCRT (endosomal sorting complex required for transport) called Alix[13]. BMP and Alix promote the budding of vesicle into the MVB lumen and its back fusion with limiting endosomal membrane. Some cell types can release intraluminal vesicles present in the LE in the extracellular medium as exosomes[14]. This is accomplished by fusion of mulitvesicular late endosomes with the plasma membrane.

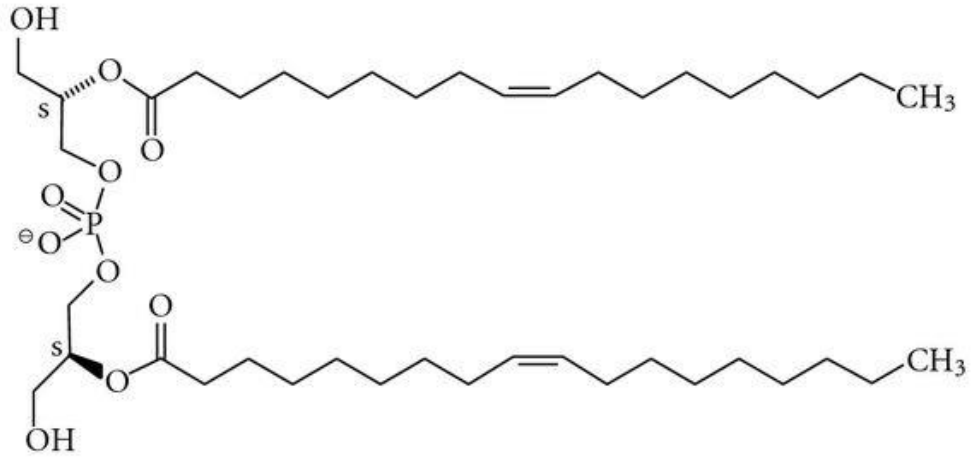

Figure 1 **Structure of BMP**. This structure represents BMP in its most prominent form 2, 2' diacyl-*sn*-1: *sn*-1' carrying oleic acid as fatty acid moiety.

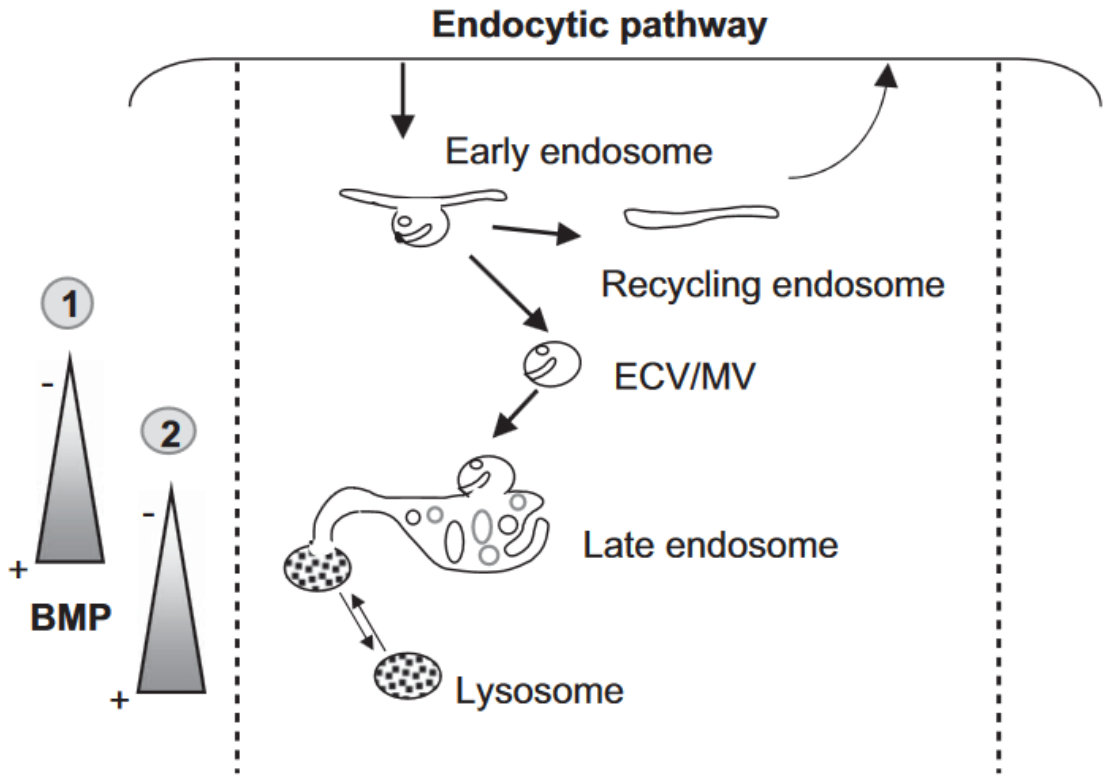

Figure 2 **Endocytotic pathway**. Extracellular materials are taken up via endocytosis and staged in the early endosome. Proteins and lipids undergo sorting and redistribution in the recycling endosome or transport to the LE by multivesicular body intermediates. 1 and 2 resemble two proposed BMP distributions. (1) Gruenberg group[15] stated that the BMP content increase from early to late endosome, but is absent in lysosome, whereas Sandhoff (2) group[16] claim that BMP increases from LE to lysosome. Graph from F. Hullin-Matsuda et al.[17]

Kobayashi et al.[18] generated a monoclonal antibody which is able to specifically react with BMP. This antibody colocalizes with the small GTPase rab7, but not with rab5, indicating that BMP is found in LE and lysosomes, but not in early endosomes. Furthermore, BMP was found to be highly enriched in membranes of the LE (~15% of total PL),specifically in intraluminal vesicles (70% of total PL)[19,20]. Moreover, they proposed that when the antibody is internalized by endocytosis in cultured BHK fibroblasts, redistribution of the multifunctional receptor for insulin like growth factor 2 (IGF2) and ligands bearing mannose 6-phosphate from trans-golgi network (TGN) to late endosome occurs. The sorting of this multifunctional receptor is one of the important functions of the LE, as it delivers newly synthesized lysosomal enzymes, which carry the mannose-6-phosphate signal, from the TGN to late endosomes.

Accordingly, they suggested that BMP-rich membranes affect protein-sorting. Furthermore, they reported that LEs play a key role in cellular cholesterol distribution to the plasma membrane and other compartments. Interestingly, accumulation of the antibody led to an increase in cholesterol levels in the LE, which indicates that selective perturbation of BMP-rich membranes affects the regulation of intracellular cholesterol transport.

The degradation of sphingolipids and glycosphingolipids takes places in the LE/lysosome, where BMP functions as a stimulator of sphingolipid degradative enzymes[21]. Acidic hydrolases catalyze the release of monosaccharides from glycosphingolipids in a sequential fashion. In order to make the glycolipids accessible to the enzymes, five activator proteins (GM2 activator protein) and four sphingolipid activator proteins (SAP A-D) act on the surface of intra-endo/lysosomal membrane vesicles. Interaction of SAP C with BMP induces fusion of BMP containing membranes at acidic pH. Notably, the absence, or mutations of these activators is reported to cause phospholipdosis[22]. High BMP and low cholesterol content in certain areas of the internal membrane stimulate the degradation of glycolipids by hydrolases[23]. Furthermore, BMP is shown to interfere with some enzyme activities (β-galactosidase and β-glucosidase) in lysosomal fractions[24]. Another enzyme that is reported to show increased activity in the presence of BMP is the lysosomal acid lipase (LAL)[25]. LAL is essential for the degradation of cholesteryl esters and triacylglycerol, which are delivered to the lysosome by lipoproteins.

1.2. BMP Synthesis

BMP is a structural isomer of phosphatidylglycerol (PG) with a *sn*-1 glycerol phosphate ester and one acyl group attached to each of the glycerol moieties[5]. Since its discovery in 1967, the underlying mechanism of BMP synthesis remains elusive. In 1991 Thornburg et al.[26] (Figure 3) proposed a synthesis route, where the conversion to BMP is initialized by the hydrolysis of PG, catalyzed by a lysosomal PLA_2, to form 1-acyl-*sn*-glycero-3-phospho-*rac*-glycerol (LPG). Subsequently, the head group glycerol is acylated on the *sn*-3: *sn*-1′ LPG with an acyl group from a

donor phospholipid revealing *sn*-3*: sn*-1' BMP. The phosphoryl ester is then reoriented from the *sn*-3 to the *sn*-1 position, liberating the *sn*-1 linked acyl chain leading to the formation of *sn*-1: *sn*-1' LPG. The final step is a second transacylation to incorporate an acyl chain into the free backbone glycerol of *sn*-1: *sn*-1′ LPG. Heravi and Waite[27] adapted this proposed mechanisms by claiming that the second step utilizes LPG rather than a diacyl phospholipid as an acyl donor, leading to the formation of glycerophosphoglycerol (GPG) and BMP. However, they also admit that a LPG utilizing a transacylase (TA) is not able to attach PUFAs to the *sn*-3: *sn*-1' LPG backbone. Therefore, they claim that a separate synthesis route for PUFA species must exist.

Another possibility of synthesizing BMP was introduced by Blitterswjik et al.[28] who proposed that phospholipase D (PLD) is able of transphosphatidylation reactions (Figure 4). Thereby, diacylglycerol (DG) generated by phospoholipase C (PLC), serves as the primary alcohol reacting with a phosphatidyl-PLD intermediate. This process leads to the formation of Bis diacylgly.(BDP), which is subsequently deacylated to BMP by $PLA_{1/2}$[28].

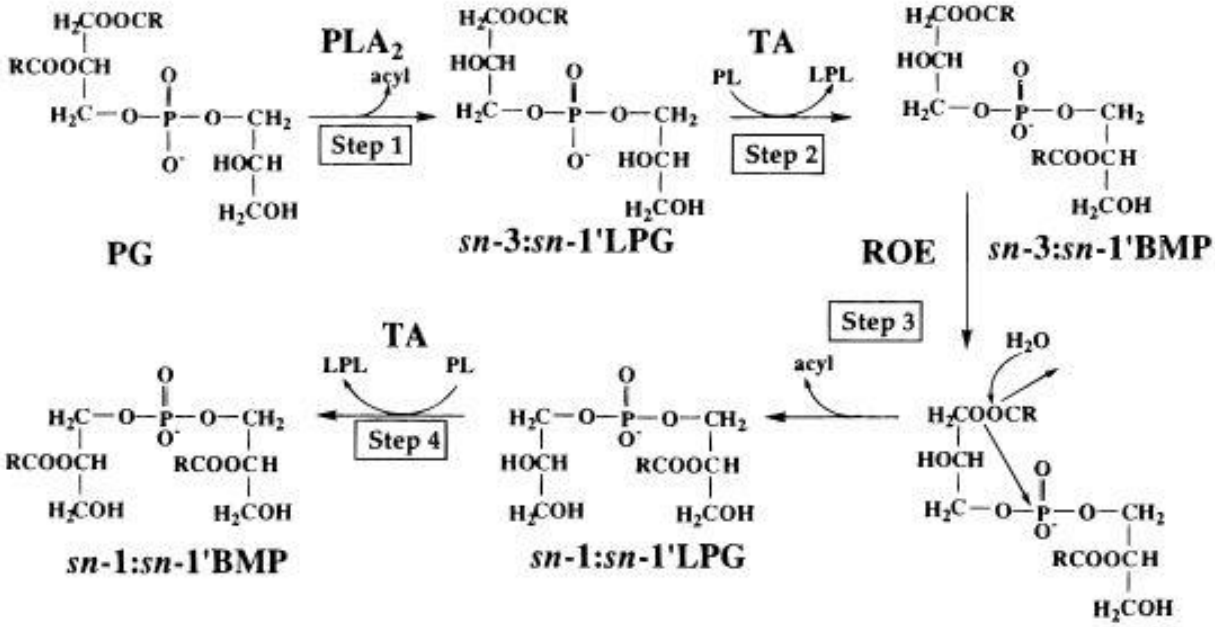

Figure 3 **BMP synthesis route with PG as precurosr**. PLA_2 catalyzes the hydrolysis from PG to *sn*-3: *sn*-1' LPG. LPG is then transacylated using diacyl phospholipids forming *sn*-3: *sn*-1'BMP.

A reorientation at the glycerol backbone leads to the formation of *sn*-1: *sn*-1' LPG. The last step requires a transacylation using again diacyl phospholipids to form *sn*-1: *sn*-1'BMP. Graph from Heravi and Waite[27].

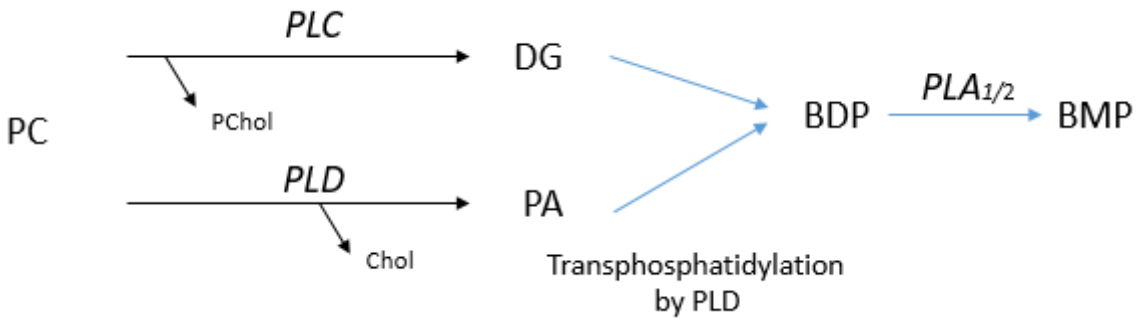

Figure 4 **Transphophatidlyation catalyzed by PLD**. PC is converted to DG and choline phosphate (PChol) by PLC, or PA and choline (Chol) by PLD. In the presence of a primary alcohol, like DG, PLD mediates the formation of BDP by attaching DG to PA in a transphosphatidylation reaction. Subsequently, BDP can be converted to BMP by $PLA_{1/2}$.

1.3. BMP Degradation

Due to the unique stereoconfiguration of BMP, it cannot be degraded by lysosomal phospholipases. Pribasnig et al.[29] provided evidence that α/β hydrolase domain-containing 6 (ABHD6) is responsible for 90% of the BMP hydrolase activity in the liver. They reported increasing hepatic BMP levels after knockdown of ABHD6. ABHD6 does not show acid hydrolase activity implicating that BMP is degraded after export from the acidic organelle. Besides ABHD6, the capability of degrading BMP in-vitro was found by a member of the carboxylesterase family[30], pancreatic lipase related protein 2 (PLRP2)[31], and ABHD12[32]. Recently, ABHD12 has been identified to exhibit lysophosphatidylserine hydrolyzing activity in mouse brain, which may contribute to BMP hydrolysis in brain because mice lacking ABHD12 show a ~2-fold reduction in BMP hydrolyzing activity at pH 7.5[32]. ABHD12 is highly expressed in the brain and barely present in the liver, which could explain the high ABHD6-independent BMP hydrolyzing activity detected in brain but not in liver lysates. PLRP2 has a broad substrate specificity and is expressed in the pancreas, but might

also possess intracellular functions. It hydrolyzes triglycerides, phospholipids, and galactolipids and is involved in T cell-mediated cytotoxicity and dietary fat absorption [31].

1.4. BMP in Disease

BMP accumulation was observed in many genetic lysosomal storage disorders (LSD)[33–38]. LSDs are a group of rare, inborn, metabolic disorders characterized by deficiencies in lysosomal enzymes or transport proteins leading to intralysosomal accumulation of undegraded substrates. LSDs comprise a group of ~ 70 monogenic disorders of lysosomal catabolism. These disorders are caused by mutations in genes encoding lysosomal proteins, such as lysosomal glycosidases, proteases, integral membrane proteins, transporters, enzyme modifiers or activators. Mutations in lysosomal genes alter the function of the encoded protein, resulting in lysosomal dysfunction and the steady accumulation of substrates inside the lysosome, which finally can lead to cellular malfunctions and cell death. The stored and accumulated material is usually the substrate of the deficient enzyme, for example, glycosaminoglycans in mucopolysaccharidoses, sphingomyelin and cholesterol in Niemann-Pick type A/B or C, and glycolipids in Gaucher and Fabry disease. There are approximately 1300 genes involved in lysosomal function, of which many have been as associated with monogenic disorders. These include 50 enzyme deficiencies, which can be sub-classified according to the type of stored material into 7 disorders involving integral membrane proteins, 14 disorders involving the production of lipofuscin, and 12 disorders of lysosomal organelles[33,39–44].

Niemann-Pick diseases (NPD) are well documented regarding altered BMP levels, as not all LSDs display accumulation of BMP. NPD is divided into three types: Niemann-Pick disease type A (NPA), type B (NPB), and type C (NPC). NPA and NPB display acid sphingomyelinase deficiencies, whereas NPC is resulting from deficiency of NPC1, or NPC2 transport protein. Notably, NPC shows the biggest impact on BMP levels. Besides being a lysosomal storage disorder, NPC is also an endosomal storage disorder[45]. Interestingly, BMP accumulates in liver and spleen from patients

with NPD, but no BMP increase in the brain was found, although NPDs are associated with neurological diseases[34,35,46,47].

Another LSD, where changes in BMP have been reported, is neuronal ceroid lipofuscinoses (NCL), which is a group of neurodegernative lysosomal disorders present in infantile and juvenile forms. Here, BMP is elevated in the brain of infantile, but not the juvenile NCL[46,48].

As metioned before, not all LSDs show accumulation of BMP, but some display augmentation of cellular BMP levels, for instance mucopolysaccharidosis I and II, NP type A/B and Fabry diseases. Furthermore, Meikle et al.[36] measured BMP levels in fibroblasts from patients with eight different LSDs. They observed only very moderate increases in BMP levels, compared to the tissue of patients. Also, patients with LSDs showed a cell/tissue specific BMP release, as serum lipoproteins carrying BMP were found in macrophages and the liver, but not in the brain. Brotherus et al.[49] observed that most of the lysosomal disorders are associated with LE and lysosome proliferation, thus leading to an increase of BMP. However, LE and lysosome proliferation cannot be the only cause of BMP accumulation, as there are cases were the amount of BMP in diseased tissues of patients was much smaller/not elevated in relation to the amount of organelles in these tissues[35].

In addition to genetic origin, LSD can also be induced as side effects of cationic amphiphilic drugs (CADs). These drugs cause lipid accumulation in spleen, liver and other tissue, designated as drug-induced phospholipidosis (DIPL) [51]. So far, over 50 marketed and experimental CADs have been reported to induce phospholipidosis. Muehlbacher et al.[52] screened 297 CADs and CAD-like compounds for their ability to induce phospholipidosis. Some clinical relevant CADs that induce phospholipidosis are shown in Table 1. CADs are reported to increase or induce acidic phospholipid accumulation, especially BMP. Accordingly, PL analysis of amiodarone-treated rat samples identified BMP as a biomarker of phospholipidosis[53]. Amiodarone (Figure 5) is considered as prototypical CAD. It is an iodine-rich benzofuran derivative which is categorized as a class III antiarrhythmic drug. Amiodarone blocks the myocardial calcium, potassium and sodium channels in cardiac tissue, resulting in prolongation

of the refractory period and cardiac action potential. Amiodarone has many side effects if administered on a chronic basis involving DIPL[54–56].

The underlying mechanism of the CAD induced phospholipidosis is not fully understood. CADs accumulate in the LE/lysosome and form drug-lipid complexes with BMP, which impairs lysosomal phospholipase activity[57,58]. Petersen et al.[59] reported lysosomal membrane permeabilization (LMP) upon CAD treatment, which is induced by inhibition of acid sphingomyelinase. This can lead to destabilization of the lysosomal membrane by increasing sphingomyelin levels and to the release of cathepsins (lysosomal proteases) into the cytosol resulting in the digestions of vital proteins and cell death.

LMP is mainly associated with apoptosis and apoptotic signaling. Cathepsins cause the proteolytic activation of the B-cell lymphoma-2 family protein Bid, which then induces mitochondrial outer membrane permeabilization (MOMP), which constitutes one of the major checkpoints of apoptotic cell death. MOMP triggers the release of cytochrome c, which contributes to the activation of caspases. Caspases are proteases that are responsible for the degradation of nuclear and cytoplasmic proteins. However, cathepsin release may result in caspase-dependent or -independent cell death with or without involvement of mitochondria[60]. Moreover, PLA2, sphingosine kinase-1, and the B-cell lymphoma-2 family proteins Bcl-2, Bcl-X_L, and induced myeloid leukemia cell differentiation protein (Mcl-1) may all be downstream targets of cathepsins. Additionally, massive lysosomal rupture induces the release of the entire content of the lysosome causing cytoplasmic acidification and hydrolysis of cytoplasmic compounds, which may have lethal consequences for the cell[61]. Besides lysosomotropic detergents like CADs, LMP can also be caused by an increase in free-radicals levels, emerging from hydrogen peroxide reacting with intralysosomal iron[62,63].

Table 1 List of common CADs that induce DIPL.

Name	Type
Amiodarone	Anti-arrythmic
AY-9944	Anti-hyperlipidemic
Chlorpromazine	Anti-psychotic
Fluoxetine	Anti-depressant
Imipramine	Anti-depressant
Tamoxifen	Anti-estrogenic
Chloroquine	Anti-malarial
Tacrine	Cholinesterase inhibitor

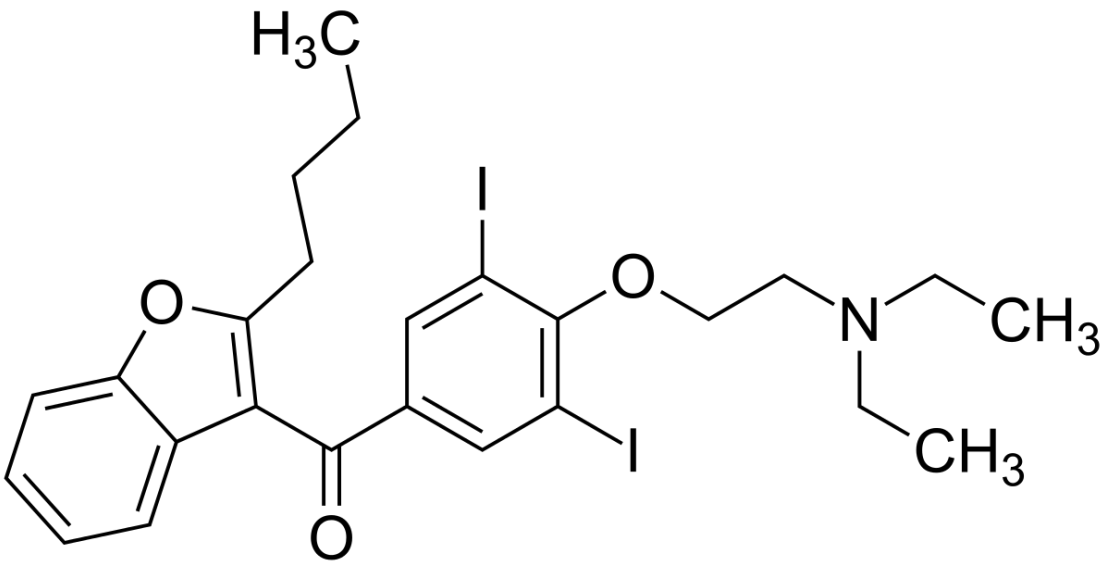

Figure 5 **Structure of amiodarone**. The structure of amiodarone presented in its uncharged state. If the CAD enters the lysosomes it is protonated on the nitrogen atom and forms a drug-lipid complex with BMP.

1.5. Hypothesis and Aims

We hypothesize that exploring BMP synthesis will provide important information about the physiological and pathophysiological role of BMP in lysosomal cargo sorting.

Ther aims of this study are:

(i) To get basic insights into pathways regulating BMP biosynthesis.

(ii) To investigate whether increased BMP synthesis can protect from amiodarone-induced cell damage.

2. Materials and methods

2.1. Buffers, Solutions and Solvents

Table 2 Ingredient list of buffers, solutions and solvents

1000x – Protease-Inhibitor (Pi) stock	20 mg/mL leupeptine (Sigma) 2 mg/mL antipain (Sigma) 1 mg/mL pepstatin (roth)
HSL-buffer	250 mM sucrose (Sigma) 1 mM EDTA (Lactan) 1 mM dithiotreitol, pH 7.0 (Roche)
1x PBS	137 mM NaCl 2.7 mM KCl 4.3 mM Na_2HPO_4 1.4 mM KH_2PO_4, pH 7.4
Agarosegelelectrophoresis	
1x TAE buffer	40 mM Tris-HCl, pH 7.2 50 mM EDTA 7% acetic acid (Roth)
5x DNA loading dye	12% glycerin (Promega) 0.25% bromphenol blue (Merck) 0.25% xylene cyanol
SDS-PAGE	
10X tris-glycin buffer	200 Mm Tris-HCl 1.6 M glycin (Merck) 0.83% SDS (Roth)
4x Lower buffer	1.5 M Tris-HCl, pH 8.8
4x Upper buffer	0.5 M Tris-HCl, pH 6.8
4x SDS-loading dye	200 mM Tris-HCl pH 6.8 400 mM dithiotreitol 8% SDS 40% glycerine

	0.05% bromophenol blue
Coomassie staining solution	0.25% coomassie brilliant blue (Bio-Rad) 6% acetic acid 50% ethanol
Coomassie destaining solution	10% methanol 8% acetic acid
Western Blot	
CAPS Transfer buffer	10 mM CAPS (Sigma), pH 11 10% methanol
TST buffer	50 mM Tris-HCl, ph 7.4 0.1% Tween-20 (Roth) 150 mM NaCl
Transformation of chemically competent *E.coli*	
SOC-Medium	5 g/L yeast extract 20 g/L tryptone 10 mM NaCl 2.5 mM KCl 10 mM $MgCl_2$ 10 mM $MgSO_4$ 20 mM glucose
Reaction buffer	
1#Invitro BMP assay buffer pH 5.5.	50 mM Tris-HCl pH 5.5 1 mM $MgCl_2$ 1x Pi
1#Invitro BMP assay buffer pH 7.4	50 mM Tris-HCl pH 7.4 1 mM $MgCl_2$ 1x Pi
Invitro BMP assay buffer pH 5.5 For investigating basal BMP formation	50 mM acetate buffer pH 5.5 1 mM $MgCl_2$ 100 mM KCl 0.1% NP-40 2 mM DTT

	1 mM $CaCl_2$
Invitro BMP assay buffer pH 7.4 For investigating basal BMP formation	50 mM KH_2PO_4, pH 7.4 1 mM $MgCl_2$ 100 mM KCl 0.1% NP-40 2 mM DTT 1 mM $CaCl_2$
Cathepsin Buffer	50 mM sodium acetate pH 6.0 4 mM EDTA Pi

2.2. Higher eukaryotic organisms

Table 3 Cell lines used for in-vivo studies.

Cell line	Tissue/morphology	ATCC number	Media	Culture conditions
COS7 *Cercophithecus aethiops*	Kidney/fibroblast	CRL-1651	Dulbecco's Modified Eagle Medium (DMEM) 10% fetal bovine serum	37°C
AML12 *Mus musculus*	Liver/epithelial	CRL-2254	DMEM 10% FCS 0.005 mg/mL insulin 0.005 mg/mL transferrin 5 ng/mL selenium 40 ng/mL dexamethasone	37°C
RAW 264.7 Mus musculus	Abelson murine leukemia virus-induced tumor; ascites/macrophages	TIB-71	Dulbecco's Modified Eagle Medium (DMEM) 10% fetal bovine serum	37°C
C8-D1A *Mus musculus*	Brain/astrocyte	CRL-2541	Dulbecco's Modified Eagle Medium (DMEM) 10% fetal	37°C

			bovine serum	
MIN6 *Mus musculus*	Pancreatic beta cells	CVCL_0431	Dulbecco's Modified Eagle Medium (DMEM) 10% fetal bovine serum	37°C
SGBS *Homo sapiens, human*	Pre-adipocytes		0.1% gelatin for coating DMEM/F12 1% biotin 1% pantothenic acid	37°C

2.3. Lipid substrates and Inhibitors

Substrates and inhibitors utilized for cell culture and *in-vitro* assays were purchased from Avanti Polar Lipids, Fermentek, and Sigma Aldrich.

Table 4 Substrates and inhibitors used for assays and in-vivo experiments

Lipids	**Formula**	**Molecular weight**
14:0 BMP	$C_{34}H_{70}NO_{10}P$	683.894
18:1 PG	$C_{42}H_{78}O_{10}P$	797.026
16:0 PG	$C_{38}H_{74}O_{10}P$	744.952
18:1 PC	$C_{44}H_{84}NO_8P$	786.113
18:1 PA	$C_{39}H_{72}O_8P$	722.948
18:1 LPG	$C_{24}H_{46}O_9P$	532.580
Oleoyl-CoA	$C_{39}H_{68}N_7O_{17}P_3S$	1031.98
Inhibitors		
VU0155056 (PLD inhibitor)	$C_{25}H_{26}N_4O_2$	414.206
VU0285655-1 (PLD2 inhibitor)	$C_{25}H_{27}N_5O_2$	429.216
VU0359595 (PLD1 inhibitor)	$C_{25}H_{29}BrN_4O_2$	491.427
Triacsin C	$C_{11}H_{17}N_3O$	207.30
Bafilomycin A1	$C_{35}H_{58}O_9$	622.83
Fluorescents		
Nα–CBZ–Arg–Arg–7–amido–4–methylcoumarin	$C_{30}H_{39}N_9O_6$	621.69

2.4. Cell culture experiments

2.4.1. BMP synthesis in different cell lines

To investigate BMP synthesis upon PG supplementation, six different cell lines were selected. COS7, AML12, MIN6, SGBS, RAW and AST were cultivated until confluence for 24h under standard conditions as described in Table 3. Lipid substrates were prepared by dispersing PG 18:1 or other lipids in PBS by brief sonication. To initiate BMP synthesis, PG 18:1 was added (50µM final concentration). PA (50µM final concentration) and PBS (carrier) served as negative controls. After 24 h incubation, cells were washed three times with PBS, harvested by scraping off with a rubber policeman, and centrifuged at 1200 rpm for 3 min to obtain a pellet. Pellets were stored at -20°C.

2.4.2. Time dependent BMP synthesis

To examine time dependent BMP synthesis, COS7 and AML12 cells were cultivated until confluence for 24 hours under standard conditions (Table 3). PG 18:1 (50µM final concentration) was supplemented and cells were incubated for 0, 2, 4 and 6 hours. Subsequently, cells were harvested, washed three times with PBS and centrifuged at 1200 rpm for 3 min to obtain a pellet. Pellets were stored at -20°C until further analysis.

2.4.3. Concentration dependent BMP synthesis

To determine whether BMP synthesis is dose dependent, COS7 cells were cultivated until confluent for 24 hours under standard conditions (Table 3). PG 18:1 (0, 5, 10, 20, 50µM final concentration) was supplemented and cells were incubated for 6h. Subsequently, cells were washed three times with 1xPBS, harvested and centrifuged at 1200 rpm for 3 min to obtain a pellet. Pellets were stored at -20°C until further analysis.

2.4.4. PLD and ACS inhibition

To examine whether PLD or acyl-CoA synthetase (ACS) are involved in the synthesis of BMP, different inhibitors (PLD1, PLD2 and PLD), as well as Triacsin C (ACS) were tested. COS7 cells were cultivated until confluence under standard conditions (Table 3). Subsequently, PG 18:1 (50µM final concentration) and the inhibitors (Table 4

Substrates and inhibitors used for assays and in-vivo experimentsTable 4) were added simultaneously. The inhibitors were diluted in DMSO (0.1% total content in the sample) and had a final concentration of 5µM. Triacsin C, was used at a concentration of 10 µM dissolved in DMSO (0.1% final concentration) After 6 hours of incubation, cells were harvested, washed in PBS and pellets stored at -20°C for further analysis.

2.5. LDH-Cytotoxicity assays

LDH is a fairly stable enzyme and its release is an indicator of cellular decay and cell-death. LDH is an oxidoreductase enzyme that catalyzes the interconversion of pyruvate to lactate. Two different assay kits were used to assess cytotoxicity and survivability. The CytoScan™ LDH Cytotoxicity Assay provides a quantitative colorimetric method of assaying cellular cytotoxicity. The released LDH is measured with a coupled enzymatic reaction that results in the conversion of a tetrazolium salt (iodonitrotetrazolium) into a red color formazan by diaphorase. The LDH activity is determined as NADH oxidation or INT reduction over a defined time period. The resulting formazan absorbs maximally at 492nm and can be measured quantitatively at 490nm. The kit from SIGMA also utilizes the LDHs ability of reducing NAD to NADH, which is specifically detected by a colorimetric (450 nm) assay. Both kits required a standard calibration curve, which was made as described by the supplied manual. Furthermore, both kits needed 20 µL of lysate/supernatant to be mixed with 200 µL of the provided substrate mix. Incubation time was dependent on the amount of LDH in the sample. A dilution of the sample must be considered if the base signal is above the linear range.

2.5.1. CAD-induced cytotoxicity determination

COS7 cells were cultivated until confluence under standard conditions (Table 3). Subsequently, PG 18:1 was supplemented (50µM final concentration). PBS was used as a carrier and utilized as a negative control. After 24 hours, cells were washed 3x with PBS and fresh DMEM (no FCS) was applied. Next, different concentrations of amiodarone were added (0, 0.2, 2, 20, 200, 400 µM and 0, 1, 2, 5, 10, 20 µM) and incubation continued for 12 hours. Additionally, COS7 cells treated

with 0, 1, 2, 5, 10, 20 µM amiodarone were also incubated for 24h. To obtain the 100% cytotoxicity value, cells were treated with lysis-buffer for 30 min at 37°C. Approximately 700 µL of the supernatant was transferred to a new 1.5 mL tube and centrifuged for 5min 1000x g RT. The LDH activity was determined with the CytoScan™ LDH Cytotoxicity Assay.

2.5.2. Effect of PG 16:0 on survivability

COS7 cells were cultivated until confluence for 24h under standard conditions (Table 3). Subsequently, PG 18:1 or PG 16:0 were supplemented (50µM final concentration) and incubated for 24 hours. Next, different concentrations of amiodarone (0, 5, 20 µM) were added and incubation continued for 12h. 700 µL of the supernatant was transferred to a new 1.5 mL tube and centrifuged for 5min 1000x g. The LDH activity was determined with the LDH Cytotoxicity Assay kit from SIGMA.

2.6. Inhibition of lysosomal acidification with bafilomycin A1

COS7 cells were cultivated until confluence for 24h under standard conditions (Table 3). Subsequently, cells were either treated with PG 18:1 (50µM final concentration) or PBS. 100 nM bafilomycin A1 or the equal amount of DMSO (carrier) were added simultaneously and incubation continued for 3.5h. Cells were washed three times with PBS and centrifuged at 1200 rpm for 3 min at RT to obtain a pellet. Pellets were stored at -20°C until further analysis.

2.7. Cathepsin B detection

Cathepsin B is a lysosomal protease, which is released in the cytosol upon permeabilization of the lysosome. The amount of enzyme released can be detected by a reaction with a fluorescent substrate, where the fluorophore will be cleaved off. Therefore, COS7 cells were cultivated until confluence under standard conditions (Table 3). Subsequently, cells were washed 3x with PBS. Cells were harvested in

1mL HSL+Pi. To preserve cellular organelles, cells were disrupted using dounce-homogenization by moving the 1.5 mL tube up and down 5 times. The homogenized cells were centrifuged for 10 min 1000g. The supernatant was transferred in new 1.5 mL with the lid cut off and centrifuged at 100000g. Approximately 250µL were collected, which resembled the cytosolic fraction. 50 µL of the cytosolic fraction were then transferred to a black 96-well plate. 50 µL cathepsin buffer (Table 2) containing 20µM of the fluorescent substrate Z-Arg-Arg-7-amido-4-methylcoumarin was added. Kinetics were measured over a time course of 30 min on a Glomax Multi fluorescent plate reader (Promega, Madison, WI) at the excitation wavelength of 348 nm and the emission wavelength of 440 nm.

2.8. Protein Analysis

For calorimetric protein concentration determination, either Pierce^{TM} BCA Protein Assay kit (Thermo Fisher Scientific, USA) or Bio-Rad Protein Assay kit (Bradford 1976, Bio-Rad, Hercules, California, USA) is used. Both kits require a calibration curve, measuring six to eight 1:2 dilution prepared out of 2 mg/mL bovine serum albumin. For samples without detergent, the kit from Bio-Rad was used, as detergents interfere with the Bradford-reagent. To stay in the linear range, cell lysates might need to be diluted before 20 µL are pipetted on a 96-well plate. Bradford-reagent is diluted 1:5 with ddH_2O and 200 µL are added to the lysates. After 10 min incubation, absorbance was measured at 592nm in the plate reader (Amersham Bioscience, Uppsala, Sweden). The BCA kit was used for samples containing detergent. The BCA reagent consists out of 50 parts solution A and 1 part solution B. 200 µL of the prepared reagent is added to 20 µL of pre-diluted cell lysates on a 96 well plate and absorbance measured at 592 nm.

2.9. BMP analysis

In order to analyze BMP, lipids were extracted using either the Folch or MTBE method.

2.9.1. Folch extraction

The Folch-method is a gold standard for lipid extraction[64]. The solvent is prepared out of chloroform and methanol in a 2:1, v/v ratio. The method was adapted to suite mass-spectrometric analysis by adding 1% acetic acid, 500 nM BHT and 150 pmol of internal BMP standard. Acetic acid functions as a proton donor, for the formation of adduct-ions, which are detected by the mass spectrometer. 4 mL of the Folch solvent was added to the sample and mixed at room temperature for 120 min. After the addition of 800µL dH_2O mixing continued for 30 min. Phase separation was achieved by centrifugation at 2800 rpm. The organic lower phase was transferred to a new pyrex-tube. The remaining upper phase, 2.5 mL chloroform, mixed for 30 min and centrifuged at 2800 rpm. The two organic phases were pooled and evaporated under a stream of nitrogen. Lipids were resolved in 200-500 µL methanol/isopropanol/H_2O (30:15:5) and transferred into HPLC vials. The upper phase was evaporated in the oven at 60°C and resolved in 500 µL NaOH/SDS for protein determination.

2.9.2. MTBE extraction

For the MTBE-method, samples were extracted in 700 µL MTBE-mixture containing MTBE:methanol (3:1), acidic acid (1%), BHT (500nM) and internal BMP standard (150 pmol). Two 5 mm steel beads were added and samples were put on a Retsch TissueLyser (Qiagen, Venlo, NL) for 2x10 sec. The procedure continued with 30 min shaking on the thermomixer at full speed. 140 µL dH_2O were added for a total volume of 840 µL. Incubation continued for 10 min at full speed. Subsequently, samples were centrifuged for 5 min at full speed to achieve phase separation. The upper phase (containing the lipids) was transferred to a new vial and evaporated under a stream of nitrogen. The lipids were finally resolved in 200-500 µL methanol/isopropanol/H_2O (30:15:5) and transferred into HPLC vials. The lower phase was evaporated and resolved in 500 µL NaOH/SDS for protein determination.

Table 5 Lipid acquisition for LC-MS analysis

Name	Composition	Precursor	Product	Collision energy (eV)	Dwell time (ms)
BMP 28:0	14:0/14:0	667.45	285.3	23	150
BMP 36:2	18:1/18:1	792.58	339.3	23	150
BMP 36:3	18:1/18:2	790.56	339.3	23	150
BMP 36:4	18:2/18:2	788.54	337.3	23	150
BMP 38:5	18:1/20:4	814.56	361.3	23	150
BMP 38:6	18:2/20:4	812.55	361.3	23	150
BMP 38:6_2	18:0/22:6	812.55	385.3	23	150
BMP 40:7	18:1/22:6	838.56	385.3	23	150
BMP 40:8	20:4/20:4	836.54	361.3	23	150
BMP 40:8_2	18:2/20:4	846.54	385.3	23	150
BMP 44:12	20:4/20:4	884.54	385.3	23	150
Hemi BMP 54:3	18:1/18:1/18:1	1057.2	603.7	17	150
BDB 72:4	18:1/18:1/18:1/18:1	1321,00	603,60	20	150
PG 36:2	18:1/18:1	792.50	603.5	14	150

2.9.3. LC-ESI-MS

The Acquity Ultra Performance LC from Waters instruments (Milford, MA, USA) coupled with an Evoq Elite ER from Bruker (Billerica, MA, USA) triple quadrupole mass spectrometer system was used for BMP analysis. A Kinetex C18 column (pore diameter 82-102 Å; 1.7 µm particle size) from Phenomenex (Torrance, California, USA) was mounted onto the UPLC. Mobile phase A) was methanol/H_2O (1:1 v/v) with 1% ammonium acetate (1M), 0.1% formic acid and 8 µM H_3PO_4 . Mobile phase B) was 2-propanol with the same additives as mobile phase A. Compounds were eluted using a 0-30% gradient mobile phase B from 2min to 21 min, followed by a column wash of 100% mobile phase B from 21min to 22.30min. Subsequently, the column was re-equilibration with 100% mobile phase A from 22.35min to 25min. The flowrate was set to 0.300 ml/min. The mass spectrometer was tuned on electron spray

ionization in the multiple reaction monitoring (MRM) mode. The system was set to positive mode with a spray voltage of 3500V. The cone temperature was 350°C and the cone gas flow 20 AU. Nitrogen was used as a collision gas. The precursor and product ions for the examined BMP species are given in Table 5. The data was analyzed using the Bruker MS workstation.

2.10. In vitro-Assays

2.10.1. In-vitro BMP synthesis

For determination of BMP synthesizing activity in COS7 cell lysates, cells were washed with ice-cold PBS and disrupted by brief sonication in assay buffer according to Table 1. Lysates were centrifuged at 1000 × *g* for 10 min at 4 °C, and the supernatant was used for measuring BMP synthesizing activity. Subsequently, lysates supplemented with either PG (50µM) ± oleoyl-CoA (50 µM) were incubated on the shaker at 800 rpm for 1h at 37°C. BMP was directly extracted from the reaction mixture using the MTBE method and analyzed by mass spectrometry.

2.10.2. Determination of basal BMP synthesis

COS7 cell lysates were buffered according to Table 1. Subsequently, active lysates and heat-inactivated lysates were incubated for 2h at 37°C/800rpm. As a second control, lysates were incubated on ice for 2h. Heat inactivation was performed at 98°C for 10 minutes. Lipids were extracted using the MTBE method and BMP content was determined utilizing mass spectrometry.

2.10.3. BMP synthesis in RAW macrophages

RAW macrophages were cultivated until confluence under standard conditions (Table 2). The medium was replaced with DMEM+1% heat inactivated FCS and cells were incubated for 12h. Subsequently, the medium was collected and centrifuged for 10min at 1000x g at RT. The supernatant was set to a pH of 7.4 with HEPES (20mM final concentration). 1 mM $CaCl_2$ and 50µM PG were added to the medium.

DMEM+1% heat inactivated FCS was used as a negative control. Additionally, a separate reaction mixture was prepared containing conditioned medium, 50 µM PG ± 2.5 mM EDTA. The reaction mixtures were put onto the shaker at 800 rpm 37°C and the reaction was stopped after 0h and 4h. The reaction at timepoint 0 was heat inactivated at 98°C for 10 min. Lipids were extracted using the MTBE-method (2.9.2) and analyzed by LC-ESI-MS.

2.11. Fluorescent microscopy

Microscopy was performed using a Leica SP5 confocal and 2-photon microscope with spectral detection (Leica Inc., Germany) as well as a Leica HCX PL APO 63x NA 1.4 OIL immersion objective. Cells were stained using SYTOX green (Invitrogen, Inc.; final concentration 100nM). SYTOX green was excited with a 2-photon laser source and emission detected using appropriate filters.

2.12. Statistics

All results were expressed as mean±SD. Statistical significance of data was analyzed by the two-tailed Student's t -test between the PG supplemented and normal cells. For statistical analysis of the differences among group means, we performed one-way, or two-way ANOVA followed by Bonferroni, or Dunnett multiple comparison post hoc test. Values of $p<0.05$ were considered statistically significant.

3. Results

3.1. BMP synthesis

3.1.1. PG – induced BMP synthesis in different cell lines

PG has been identified as precursor of BMP and can induce BMP formation in different cell lines. In order to examine BMP synthesis, a cell line featuring high BMP synthesis upon treatment with PG is favorable. Six different cell lines (Table 3) were treated with PG to induce BMP formation. PA and PBS (carrier) –treated cells were used as a control. Cells were harvested after 24h treatment and BMP content was determined by mass spectrometry. RAW macrophages exhibit the highest basal BMP levels among the tested cell lines. In the presence of PG, COS7 cells show highest increase in BMP concentration (>100 - fold increase compared to the PBS control), followed by AST (>5 - fold), Min6 (>5 - fold), RAW (3 – fold), SGBS (3 – fold) (Figure 6). In contrast, AML12 cells show no BMP synthesis upon PG treatment. Furthermore, SGBS cells show a unique BMP composition, having BMP 44:12 as the major species (Figure 7c), whereas the other cell lines show BMP 36:2 as the most prominent species (Figure 7).

The incubation of cells with PG 18:1 resulted mostly in the accumulation of BMP 36:2 in all tested cell lines except SGBS cell (Figure 7c). Interestingly, SGBS synthesized BMP subspecies containing DHA (40:7 and 44:12, Table 5) indicating fast remodeling of newly synthesized BMP species.

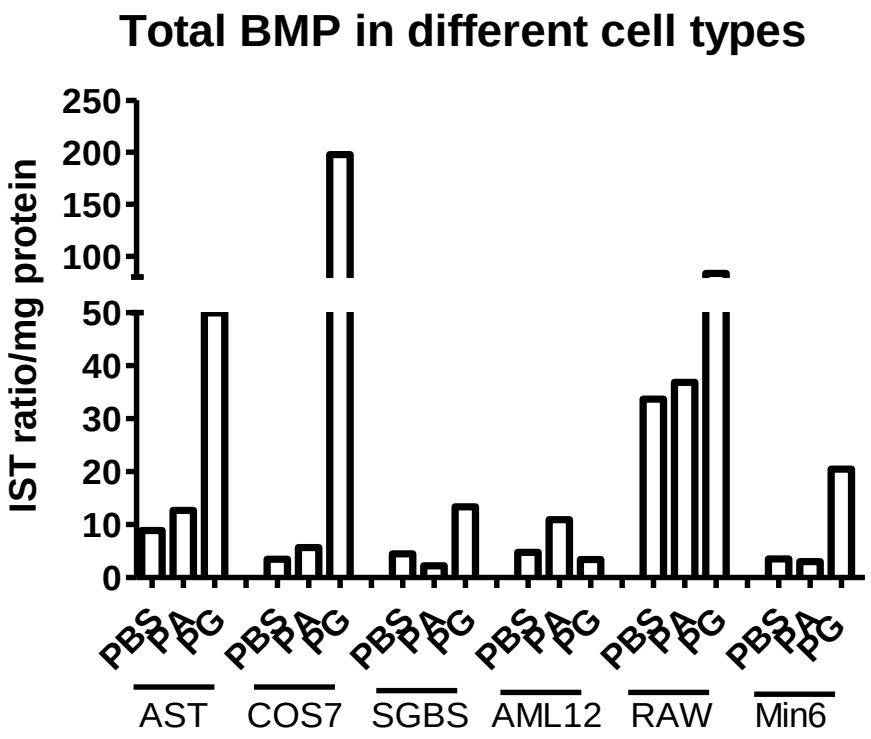

Figure 6 PG – induced BMP accumulation in different cell lines. AST, COS7, SGBS, AML12, RAW, and Min6 cells were cultured until confluence and then incubated with PG (50 μM), PA (50 μM), or PBS (carrier) for 24 hours under standard conditions (DMEM/10%FCS). Subsequently, cells were washed 3x with PBS, scrabbed off with a rubber policeman, and lipids were extracted using the Folch-method. BMP content was then determined by mass spectrometry and protein concentration was assessed using the BCA kit using BSA as standard (n=1).

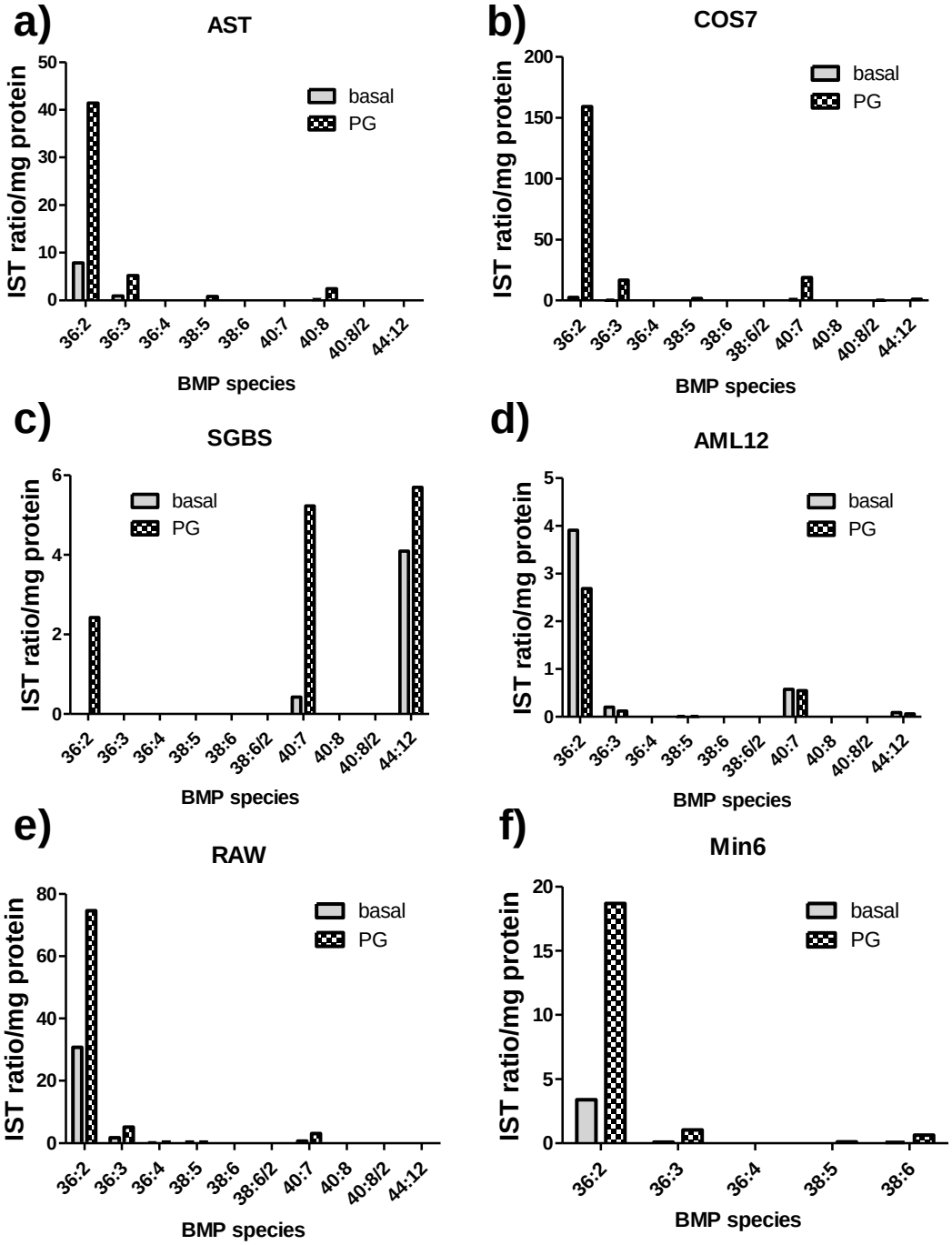

Figure 7 BMP profile of the cell lines. AST, COS7, SGBS, AML12, RAW, and Min6 cells were cultured until confluence and incubated with PG (50 μM), PA (50 μM), or PBS (carrier) for 24 hours under standard conditions (DMEM/10%FCS). Subsequently, cells were washed 3x with PBS, scraped off with a rubber policeman, and lipids were extracted using the Folch-method. BMP content was then determined by mass spectrometry and protein concentration was assessed using the BCA kit using BSA as standard (n=1).

3.1.2. COS7 but not AML-12 cells show PG-induced BMP accumulation

To confirm data shown in **Figure 6**, we studied the time and dose-dependent synthesis of BMP in COS7 cells and used AML-12 cells as negative control. PG-supplemented COS7 cells show a linear increase in BMP synthesis for at least 6h (Figure 8a). AML12 cells do not show any increase in BMP synthesis activity within this time period (Figure 8b). Cell associated PG levels also rise a time depended manner in COS7 cells (Figure 8c). AML12 also clearly exhibit increased PG levels. (Figure 8d). Yet, the intracellular PG level is ~ 10-fold lower these cells compared to COS7 cells and does not occur in a linear fashion. This indicates that the PG uptake is less efficient in AML12 cells, which might be due to a difference in uptake mechanisms. Alternatively, internalized PG is rapidly degraded and converted to other lipids than BMP. We also observed that BMP synthesis increased in a dose-dependent manner in COS7 cells (Figure 8e).

Additionally, we tested whether supplementation of free fatty acids increase BMP synthesis. In contrast to cells exposed to PG, FFA did not increase BMP synthesis (Figure 8f).This indicates that BMP synthesis is highly dependent on the presence of PG but not on FFA which can derive from PG degradation.

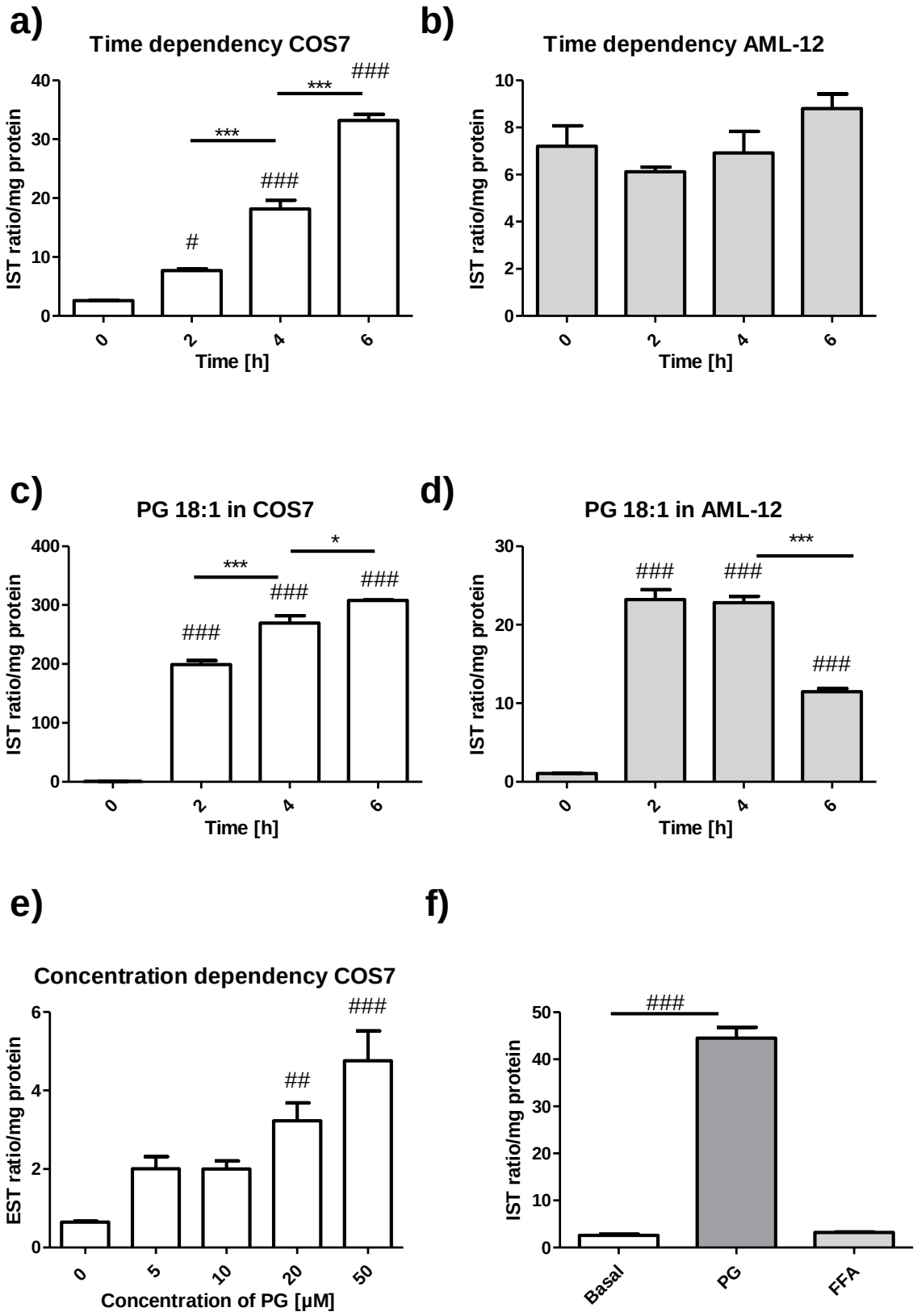
a)
Time dependency COS7
IST ratio/mg protein
Time [h]
b)
Time dependency AML-12
IST ratio/mg protein
Time [h]
c)
PG 18:1 in COS7
IST ratio/mg protein
Time [h]
d)
PG 18:1 in AML-12
IST ratio/mg protein
Time [h]
e)
Concentration dependency COS7
EST ratio/mg protein
Concentration of PG [µM]
f)
IST ratio/mg protein
Basal
PG
FFA

Figure 8 **Time and dose dependent BMP synthesis in COS7 and AML12**. For time dependent stimulation of BMP synthesis, COS7 (a,b) and AML12 (b,d) cells were cultured until confluence and then incubated with PG (50 μM) for 0, 2, 4, and 6 hours under standard conditions (DMEM/10%FCS). For dose dependent stimulation, COS7 (e) were cultured under standard conditions (DMEM/10%FCS) until confluence before treating with the indicated concentrations of PG. After 6h, cells were washed 3x and scraped off. Subsequently, cells were washed 3x with PBS, scraped off with a rubber policeman, and lipids were extracted using the Folch-method. (f) COS7 cells were cultivated as described before, but supplemented with either PG 18:1 (50μM final concentration), free fatty acids (400μM final concentration) or 1xPBS as negative control. Incubation continued for 12 hours. Cells were washed and harvested and lipids extracted using MTBE-method. BMP content was determined by mass spectrometry and protein concentration was assessed using the BCA kit using BSA as standard. Values represent mean ± SD of 3 samples. *$p < 0.05$, **$p < 0.01$, and ***$p < 0.001$; one way analysis of variance; *Bonferroni's multiple comparison test, #Dunnett's multiple comparison test.

3.1.3. Inhibition of PLD and ACS reduce BMP levels in COS7

The discovery of BMP goes back 50 years ago and since then its synthesis remains unknown. To get a basic insight into the synthetic pathways of BMP, we used inhibitors of enzymes that have been associated with BMP metabolism. PLD belongs to the phospholipase superfamily and has two intracellular isoforms (PLD1, PLD2). It uses phosphatidylcholine as substrate which is hydrolyzed to PA and choline. In the presence of DG and PC, PLD is also featuring a transphosphatidylation activity, which is leading to the formation of BDP, a putative precursor of BMP. To examine whether PLD plays a role in BMP biogenesis, cells were loaded with PG and treated with different PLD inhibitors. The general PLD inhibitor as well as PLD1 reduce BMP synthesis by 64% (PLD1) and 61% (PLD) (Figure 9, a). Inhibition of PLD2 has no significant impact on BMP synthesis (Figure 9, a).

Long chain fatty acyl-CoA synthetase (ACS) is an enzyme responsible for the intracellular synthesis of acyl-CoA that can be used for the synthesis of complex lipids or imported into mitochondria for beta-oxidation. To investigate how ACS inhibition affects BMP synthesis, cells were loaded with PG and treated with the ACS inhibitor Triacsin C. Notably, inhibition of ACS causes a 70% reduction in BMP levels. This indicates that the involvement of an acyl-CoA dependent acyltransferase in BMP synthesis (Figure 9, a).

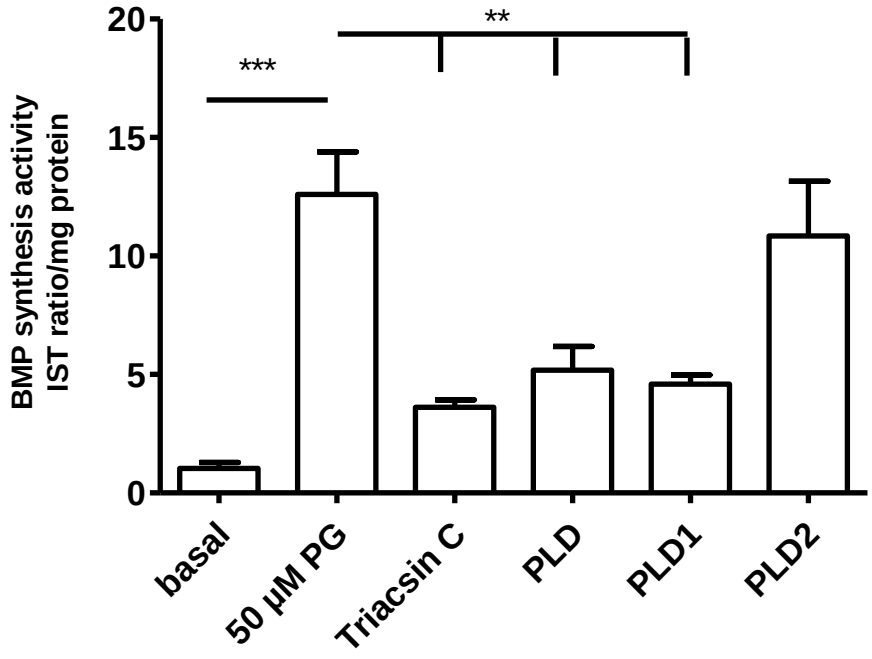

Figure 9 **Effects of PLD inhibitors on BMP formation**. COS7 cells were seeded ($3*10^5$) in 6-well dishes and incubated for 24 hours prior to the addition of PG 18:1 (50µM final concentration). The inhibitors (PLD, PLD1, and PLD2) were diluted in DMSO (0.1% total concentration) and had a final concentration of 5µM. For Triacsin C 10 µM was used. DMSO (0.1% final concentration) was used as a control. After 6 hours of incubation, cells were washed 3 times in PBS and harvested. Lipids were extracted using the MTBE-method and BMP content was determined using mass spectrometry. Protein concentration was assessed using the BCA protein detection kit, using BSA as standard. Values represent mean BMP levels ± standard deviation of 3 samples. *$p < 0.05$, **$p < 0.01$, and ***$p < 0.001$; one way analysis of variance.

3.1.4. Inhibition of lysosomal acidification does not affect BMP synthesis

Previous experiments (3.1.3, 3.1.6) demonstrated that PLD and ACS affect BMP synthesis suggesting that this process takes place rather in the cytoplasm than in acidic compartments. Yet, the cellular compartment of BMP synthesis is currently unknown. Bafilomycin A1 is a drug that disables the acidification of the lysosome by inhibition of the proton pump vacuolar-type H+-ATPase (V-ATPase). We used this drug to investigate whether reduced acidification affects BMP synthesis. We found no difference in BMP synthesis activity under basal conditions, and bafilomycin treated cells show slightly lower (10%) PG-induced BMP formation compared to cells treated with PG alone (Figure 10). This indicates that BMP formation does not require an acidic pH, thus excluding LE/lysosomes as compartments of synthesis.

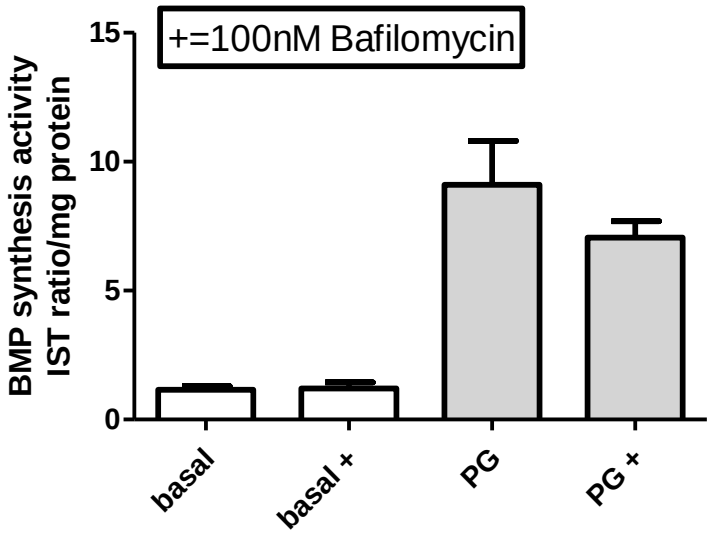

Figure 10 **Bafilomycin A1 effects on BMP synthesis**. COS7 cells were cultivated in 6 well-plates and incubated for 24h with DMEM+10%FCS. Cells were either treated with PG 18:1 (50µM final concentration) or PBS. Subsequently, 100 nM bafilomycin A1 or DMSO were added and incubation continued for 3.5h. Cells were washed three times with 1xPBS and centrifuged at 1200 rpm for 3 min to obtain a pellet. Lipids were extracted by MTBE-method and analyzed by mass spectrometry. Data are presented as mean ± S.D. of three samples.

3.1.5. Investigation of BMP synthesis in cell lysates

The inhibition of lysosomal acidification indicated that BMP synthesis rather occurs in the cytoplasm than in acidic compartments. To further investigate pH dependency and possible substrates for BMP formation, preliminary *in-vitro* assays were performed using COS7 cell lysates.

Therefore, we monitored BMP synthesis in COS7 cell lysates in the presence or absence of PG and oleoyl-CoA. Assays were performed at pH 7.4 and 5.5 resembling the pH values of cytosolic and late endosomal fractions. However, we could not detect a significant increase in BMP under the applied conditions suggesting that additional co-factors or longer incubations are required for BMP synthesis. (Figure 11).

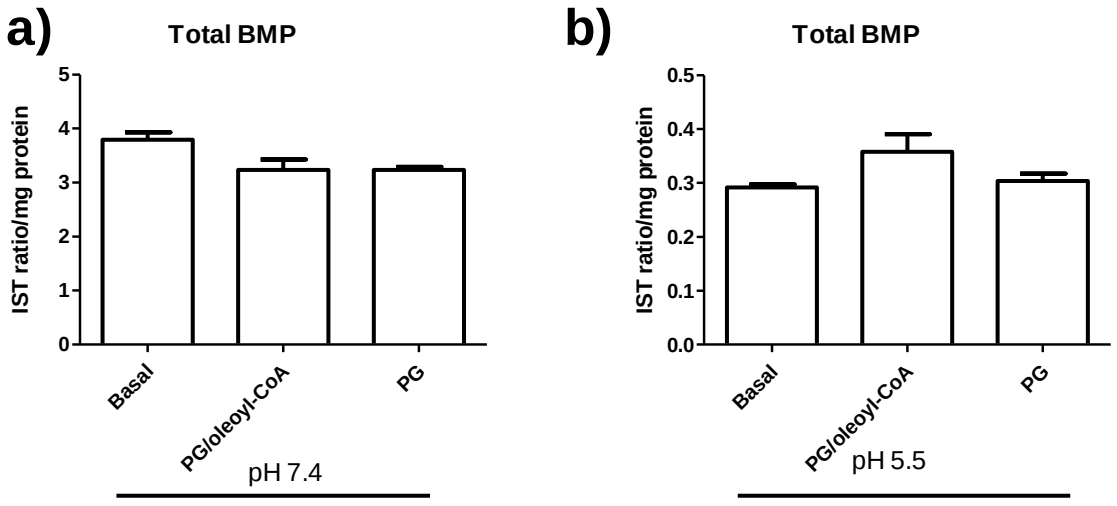

Figure 11 **In vitro BMP synthesis.** COS7 cell were sonicated in assay buffer (Table 2) at pH 5.5, and 7.4. The supernatant (1000x g) was incubated for 1h, supplemented with either PG (50μM)/oleoyl-CoA (50 μM), or solely PG. BMP was directly extracted from the reaction mixture using the MTBE method and analyzed by mass spectrometry. Values represent mean ± S.D. of 3 samples; statistical evaluation was performed using one way ANOVA).

Accordingly, the settings for the *in-vitro* assay were adjusted to longer incubation times (2h) and different buffer systems (Table 2), now including Ca^{2+} and Mg^{2+}, since many acyltransferase/transacylases require divalent ions as co-factor. In a

preliminary test, we examined the effect of the added ions on basal BMP synthesis. Heat inactivated cell lysates incubated at 37°C and cell lysates incubated on ice were used as negative controls. We found an increase in BMP levels after 2h at pH 5.5 (50%) and 7.4 (13%) compared to negative controls. (Figure 12). This indicates that BMP synthesis can occur under basal conditions at pH 5.5 and pH 7.4, and that BMP synthesis relies on mono- or/and bivalent ions. It is important to note that these assays have been performed in the absence of PG and acyl-CoA acting as acceptor or donor in the reaction. Further studies are required to investigate PG-dependent BMP formation under these conditions.

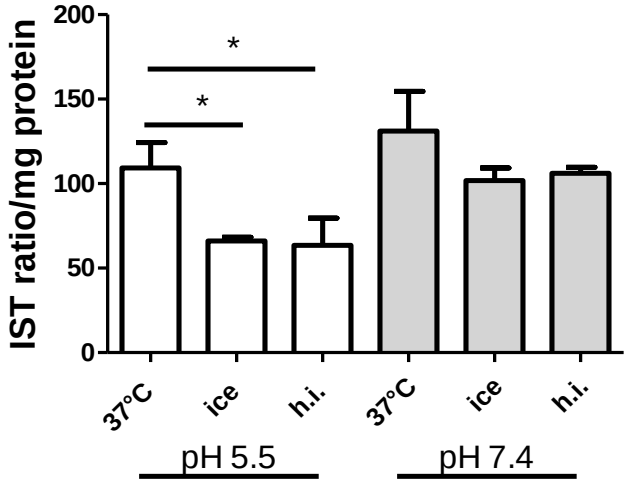

Figure 12 **Basal BMP synthesis**. COS7 cell lysates were buffered according to Table 2. Subsequently, active lysates and heat-inactivated lysates were incubated for 2h at 37°C/800rpm. As a second control, lysates were incubated on ice for 2h. Heat inactivation was performed at 98°C for 10 minutes. Lipids were extracted using the MTBE method and BMP content was determined utilizing mass spectrometry. Values represent mean BMP levels ± standard deviation of 3 samples (* $p<0.01$; one way ANOVA).

3.1.6. BMP can be synthesized extracellular

A collaboration partner suggested that BMP can be synthesized extracellularly by so far uncharacterized enzymes secreted from macrophages (personal communication with Peter Greimel, RIKEN AICS · Brain Science Institute (BSI)). To investigate whether secreted enzymes affect BMP synthesis, conditioned media of RAW macrophages were used in an *in vitro* assay. Before performing experiments with conditioned media, we had to exclude that FCS contains BMP-synthesizing activity. The cell culture medium (DMEM/1% heat-inactivated FCS) does not contain detectable BMP concentrations and incubation of medium with PG for 4h does not lead to BMP formation excluding the presence of BMP-synthesizing enzymes under the applied conditions (Figure 13a)

Conditioned media from RAW macrophages contained low amounts of BMP. Using this medium, there is a strong PG-dependent increase (>100-fold) in BMP formation after 4h of incubation (Figure 13a). This shows that BMP can also be formed extracellularly by macrophage-derived enzymes.

To narrow the search for possible, extracellular BMP synthesizing enzymes, the implication of calcium dependent enzymes were investigated. Therefore, EDTA was added to conditioned media. Total BMP is reduced by 28% upon treatment with EDTA (Figure 13, b). This indicates that divalent ions promote BMP synthesis, but addition of EDTA does not completely shut down enzyme-catalyzed BMP formation.

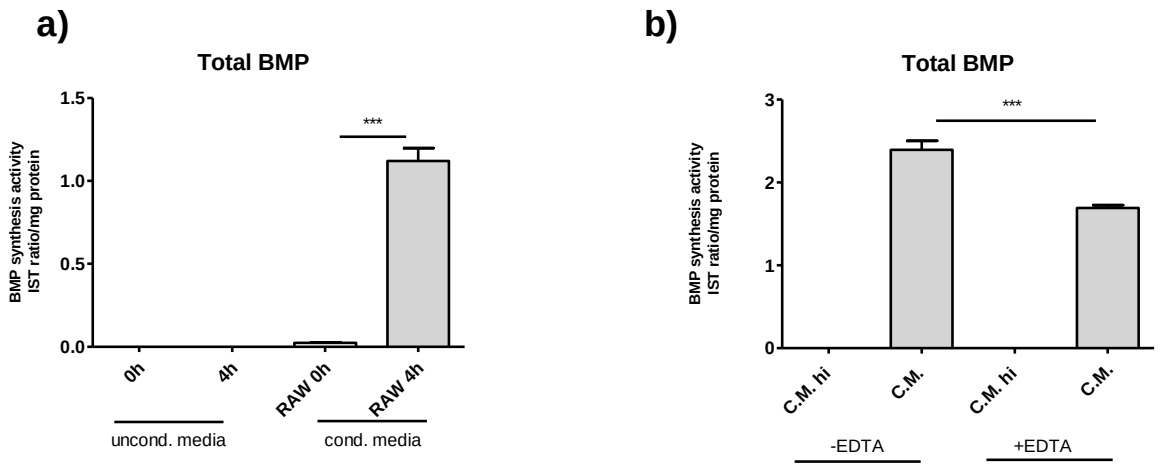

Figure 13 **Extracellular BMP synthesis**. (a) RAW macrophages were cultivated under standard conditions in DMEM/10%FCS. Subsequently, cells were washed, the medium was replaced with DMEM/1% heat inactivated FCS, and cells were incubated for 12h. The medium was collected and centrifuged for 10min at 1000g. The supernatant was set to a pH of 7.4 with HEPES (20mM final concentration, cond. medium). DMEM/1% heat inactivated FCS was used as a negative control (uncond. Media). 1 mM $CaCl_2$ and 50µM PG were added to the reaction mixtures. (b) Conditioned and unconditioned media were additionally supplemented with 2.5 mM EDTA. BMP synthesis was measured after 0h and 4h and the reaction was stopped at 98°C for 10 min. Lipids were extracted using the MTBE-method and analyzed by LC-ESI-MS . Data are presented as mean ± S.D. of three samples (*, p 0.05; **, p 0.01; ***, p 0.001; one way ANOVA).

3.2. Pathophysiological implications of BMP

3.2.1. PG supplementation reduces cytotoxic effects of amiodarone

Cationic amphiphilic drugs (CADs) accumulate in the lysosomes, causing phospholipidosis by forming drug-lipid complexes with BMP, thus inhibiting acidic phospholipase activity[57,58]. CADs strongly cause BMP accumulation in vitro and in vivo. Yet, it is unclear whether this accumulation reflects disordered BMP metabolism or if an increased cellular BMP synthesis can counteract the cytotoxic effects of CADs. Accordingly, we hypothesized that excessive BMP formation in response to PG exposure can reduce the cytotoxic effects of CADs and enhance the survivability of cells treated with amiodarone.

To test this hypothesis, we first determined cytotoxic effects of Amiodarone in COS7 cells with or without preloading with PG. Cytotoxicity was assessed by measuring LDH release into the supernatant. In the absence of PG, we observed an increase in cytotoxicity starting at 2 µM. Higher concentrations yielded in ~ 90% cell death. Notably, amiodarone showed no cytotoxic effects at 2 µM in PG-loaded cells and had also protective effects at higher concentrations.

Figure 16a indicates that the cytotoxic effects of amiodarone become evident at 2 µM and reach almost the maximum at 20 µM. In order to get a more detailed overview on the protective effects of PG preload, we limited the amiodarone concentration range from 0 to 20 µM (Figure 14b). Protective effects of PG preload were clearly observed at 2, 5, 10, and 20 µM amiodarone.

The same experiment was also conducted after longer amiodarone exposure (24h). Under these conditions, PG preloaded cells treated with 5 and 10 µM amiodarone show a 50% and 42% reduced cytotoxicity, respectively, compared to non PG-treated cells. These observations indicate that PG supplementation protects cells from amiodarone-induced cytotoxicity, but the effect diminishes at longer exposure time with the CAD.

Further examination on the protective effect of PG preload were performed by using SYTOX green as a fluorescent stain of cell permeability. This dye is impermeant to

live cells and stains nucleic acids and chromosomes of cells with leaky plasma membranes. Amiodarone-treated PG preloaded cells do not show any differences compared to control cells, whereas cells without PG preload show high accumulation of the dye, indicating severe cell damage and cell death (Figure 15). This is in line with the protective effect observed in LDH activity assays.

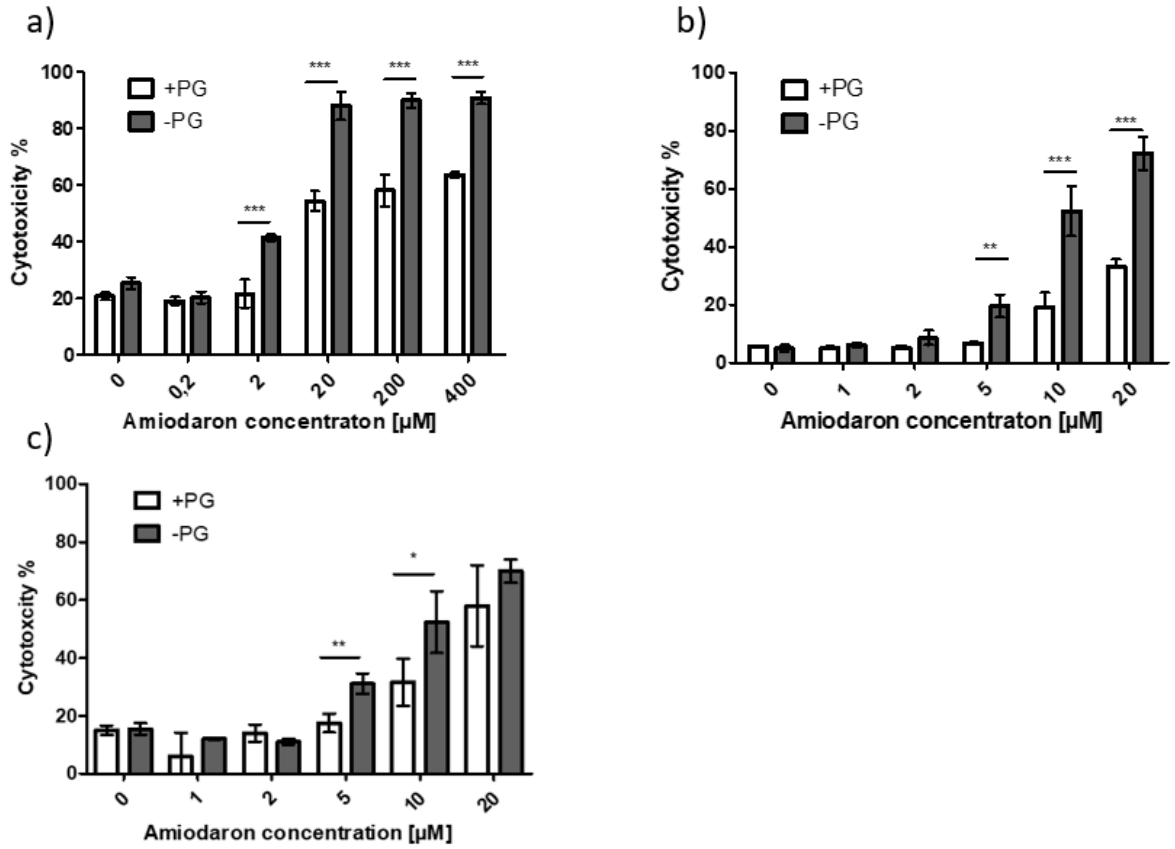

Figure 14 **Amiodarone induced cytotoxicty**. COS7 cells were cultivated ($5*10^4$) in 24 well-plates and incubated for 24h with DMEM/10%FCS in the presence or absence of PG (50µM). After this period, cells were washed and incubated DMEM containing the indicated concentrations of amiodarone and incubation continued for another 12h (a, b), or 24h (c). The supernatant was transferred into a fresh tube and LDH activity was determined with the CytoScan™ LDH Cytotoxicity Assay. To determine the 100% cytotoxicity value, cells were treated with lysis-buffer for 30 min at 37°C according to the manufactures' instruction. Data represent mean ± S.D. of three samples (*, p 0.05; **, p 0.01; ***, p 0.001; 2 way ANOVA; Bonferroni posttest???).

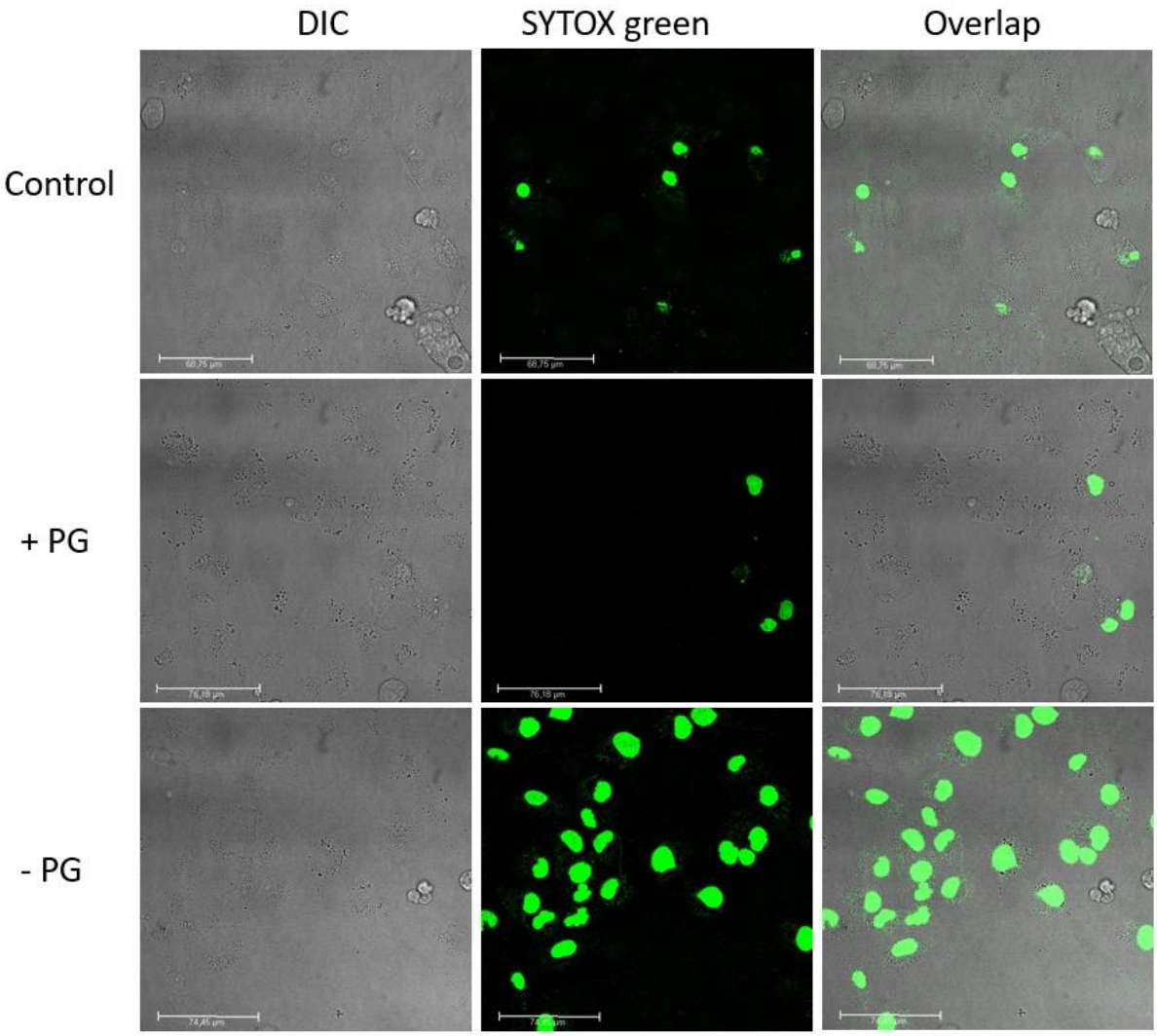

Figure 15 **SYTOX stain of cells treated with amiodarone**. COS7 cells were seeded on confocal dishes (Thermo Fisher scientific, USA) and loaded with PG for 24h under standard conditions (DMEM/10%FCS). Cells cultivated under standard conditions without PG were used as negative control. Cells were washed 3x with PBS and incubated with fresh DMEM. Subsequently 5 μM amiodarone was added and incubation continued for 6h. Cells were stained with SYTOX green for 5-10 min and examined using fluorescent microscopy

3.2.2. PG 16:0 supplementation does not protect from amiodarone - induced cytotoxicity

From the conducted studies, it is unclear whether PG or BMP is responsible for the protective effects against amiodarone-induced cytotoxicity. Therefore, we performed control experiments with PG 16:0, which cannot directly be utilized for cellular BMP synthesis[65]. In accordance with published data, our observations revealed that COS7 cells loaded with PG 18:1 showed a 45-fold increase in BMP synthesis, whereas COS7 cells supplemented with PG 16:0 showed only a 5-fold increase compared to non-loaded controls (Figure 16a).

Next, COS7 cells were supplemented with PG 16:0 or PG 18:1 and treated with amiodarone. As shown in Figure 16b, PG 18:1 but not PG 16:0 preload protects from cytotoxicity at 5 µM amiodarone. This indicates that rather BMP than PG mediates protection from CAD-induced cytotoxicity.

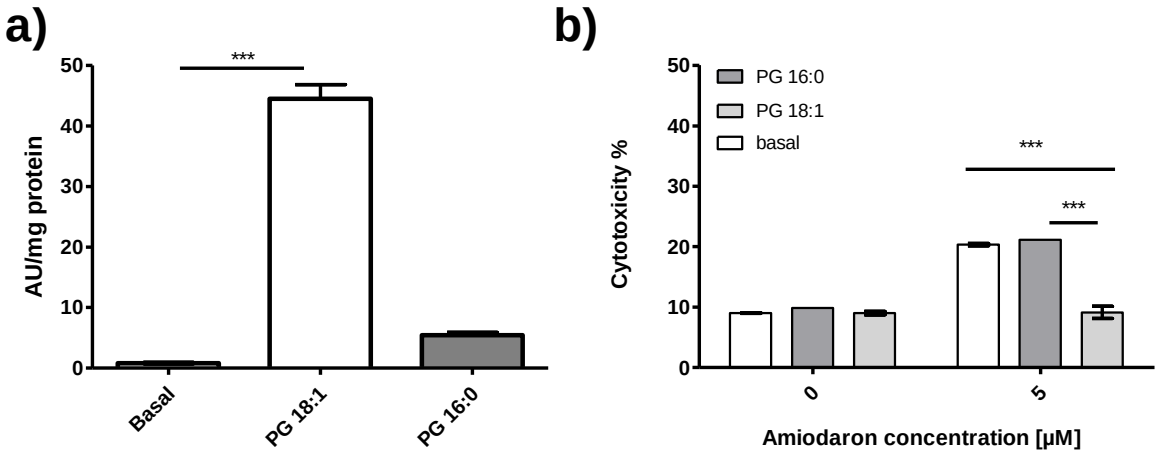

Figure 16 **Effects of different PGs on cytotoxicity and BMP synthesis**. a) Confluent COS7 cells were loaded with PG 18:1, PG16:0 or PBS and incubated for 24h under standard conditions (DMEM/10%FCS). Cells were washed 3 times with PBS and scraped off. Lipids were extracted using the MTBE-method and analyzed by mass spectrometry. b) COS7 cells were incubated under standard conditions (DMEM/10%FCS) for 24h with PG 18:1, PG 16:0 or with PBS (carrier). Cells were washed 3x with PBS and the old media was replaced with fresh DMEM. Subsequently, cells were treated with indicated amounts of amiodarone and LDH release was determined after 6h incubation using the Cytotoxicity Assay kit from SIGMA. Values represent mean ± standard deviation of 3 samples. ***$p < 0.001$; 2way ANOVA.

5.2.3. LMP is increased in cells without PG treatment

As depicted above, PG administration clearly shows protective effects on cells treated with amiodarone. However, the mechanism behind this effect remains elusive. CADs have been reported to cause lysosomal membrane permeabilization (LMP) by osmotic lysis or direct membranolytic activity in the LE/lysosomes. Petersen et al.[59] reported that CAD treatment induces LMP by inhibition of acid sphingomyelinase resulting in the accumulation of sphingomyelin, which can destabilize lysosomal outer membranes. To examine if the protective effect of PG supplementation is due to stabilization of the lysosome and thereby reduced amiodarone-induced LMP, cathepsin release was measured. Cathepsins are lysosomal proteases released in the cytosol upon damage to the lysosome, which results in the digestions of vital proteins. Therefore, increased cathepsin levels in the cytosol upon amiodarone treatment would argue for a permeabilization of lysosomal membranes. To investigate this hypothesis, a fluorescent substrate (Table 4) was utilized to detect cathepsin in cytosolic fractions of COS7 cells upon amiodarone treatment. PG pretreatment has no effect on cytosolic cathepsin activity. CAD-treated control cell show 2-fold higher cathepsin activity compared to cells preloaded with PG (Figure 17). This indicates that PG supplementation reduces amiodarone induced LMP.

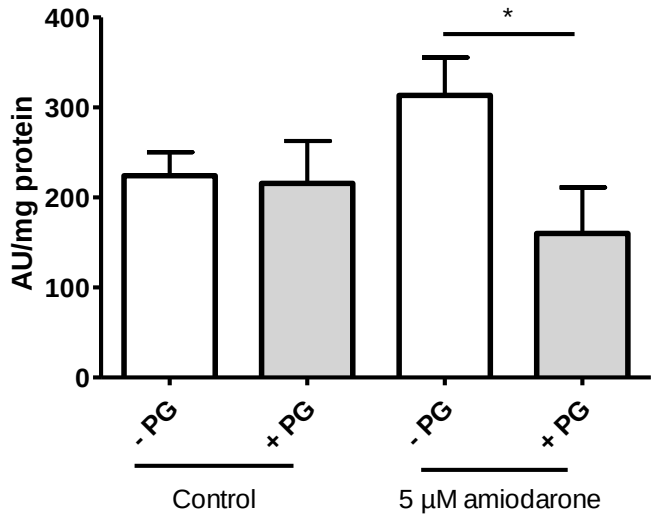

Figure 17 **PG supplementation reduces CAD-induced LMP**. COS7 cells were cultivated until confluence under standard conditions (DMEM/10%FCS.). Cells were then preloaded with ± PG and incubated for another 24h. Subsequently, cells were washed and fresh DMEM was applied prior to treatment with amiodarone (5 µM) for 6h. Cytosolic fractions were obtained as described in materials and methods (2.7). Cathepsin activity was assessed in the cytosolic fraction using a fluorescent substrate (Nα–CBZ–Arg–Arg–7–amido–4–methylcoumarin**)**. Values represent mean ± S.D (n=3). *$p < 0.01$; student's t-test..

4. Discussion

BMP is a low abundant PL, mainly encountered in LE/lysosomes, where BMP has important roles in LE/lysosomal maturation, protein-sorting and lipid degradation.[21] BMPs cone-shaped structure is reported to induce the formation of multivesicular structures, characteristic for LE[21]. Furthermore, BMP has been shown to accumulate in genetic and drug-induced LSD[66]. Despite the fact that BMP exhibits a crucial role in the regulation of lysosomal function, nothing precise is known about its synthesis. Therefore, we hypothesize that getting basic insight into the synthesis of BMP will provide important information about the physiological and pathophysiological role of BMP.

Published data suggest that PG can induce BMP synthesis in cultured cells[65]. To investigate cellular BMP synthesis, it is important to have a cell line that is able of forming BMP. We started by screening for cell lines that show BMP synthesis upon supplementation of PG assuming that PG is a precursor of BMP. Increased BMP synthesis was observed after PG supplementation in COS7, AST, RAW, Min6, and SGBS cells. The highest amount of basal BMP was present in RAW macrophages, which is in line with the literature showing that macrophages have high BMP content[7–9]. Most investigated cell lines showed increased BMP content in response to PG exposure, whereby COS7 cells showed the highest BMP synthesizing activity. PG supplementation strongly induced BMP formation in this cell line in a time and dose dependent manner. In contrast, hepatocyte-derived cell line AML12 cells did not show any PG-induced BMP formation. Currently, it is unclear why AML12 do not show an increase in BMP, which might due a difference in PG uptake or due the lack of enzymes converting PG into BMP. Alternatively, internalized PG is rapidly degraded and converted to other lipids than BMP. As BMP can be detected in AML12 cells, it can be assumed that these cells are in principal capable of synthesizing BMP independent of the availability of PG. We found that AML-12 cell internalize much lower amounts of PG compared to COS-7 cell suggesting that reduced uptake contributes to the lack of PG-induced BMP synthesis. The mechanism of PG uptake itself is also unknown. The high uptake of PG micelles by COS7 cells indicates a very efficient mechanism, which is likely mediated by a

plasma membrane receptor. Possible receptor candidates are class B scavenger receptors SR-BI and CD36 which are reported to be receptors for anionic phospholipids[56].

In most cells, exposure to dioleoyl-PG resulted in the formation of dioleoyl-BMP as major species. Another interesting observation was that SGBS cells have a different BMP profile compared to other cell lines. These cells showed a high abundance of DHA-containing BMP species indicating remodeling of newly synthesized BMP. The enzymes mediating BMP remodeling are currently unknown. A structural similar lipid is cardiolipin (CL), which undergoes remodeling after synthesis. Hullin-Matsuda et al.[67] reported that BMP formation is not affected by mutations in tafazzin, an enzyme implicated in the deacylation-reacylation cycle of CL.

So far, two mechanisms of BMP synthesis have been proposed. Thornburg et al.[26] reported that BMP is synthesized utilizing a PG precursor, whereas Blitterswjik et al.[28] stated that BMP is formed by a transphosphatidylation reaction mediated by PLD. Both mechanisms rely on PLs as precursors. To gain basic insights into the pathways involved in BMP synthesis in COS7 cells, we used specific inhibitors of PLD. Blitterswjik et al.[28] proposed that during the transphosphatidylation reactions PLD transfers PC-derived PA to DG (see Figure 4). This process is leading to the formation of BDP, which is subsequently deacylated to BMP by $PLA_{1/2}$[28].

Intracellular PLD activity is provided by two different enzymes, PLD1 and PLD2. We observed that only PLD1 decreases BMP formation in COS7cells. Yet, based on our observations no statement about the direct implication of the transacylase reaction in BMP synthesis can be made. PLD1 is mainly found at the Golgi complex, endosomes, lysosomes, and secretory granules, whereas PLD2 is present at the plasma membrane. The localization of PLD1 at LE/lysosomes implicates that PLD1 can produce BMP on the outer membrane of these organelles. Yet, PLD1 has been reported to play numerous roles in survival signaling, cell polarity, Ras activation, and maintaining autophagic flux via regulating autolysosome formation[68,69], whereas PLD2 is known to be implicated in cell proliferation, cell growth signaling, and vesicle trafficking[70–72]. Thus, PLDs are crucial enzymes in intracellular signal transduction and PLD1 may also indirectly affect LE formation and BMP synthesis via signaling pathways.

PLD is also involved in PG synthesis[73], a precursor of BMP, but we observed that PLD1 inhibitor reduced BMP synthesis under condition where PG formation is not-rate limiting. Thus, our data indicates that PLD induced BMP formation rather by transacylase reactions or promoting ILV formation than by increasing PG production.

There are two possible ways of attaching an acyl group to the non-esterified glycerol of PG or LPG, acting as precursor of BMP. An acyl group can either be transferred to an acceptor like LPG by transacylases, or by an acyl-CoA dependent acyltransferase. By inhibition of ACS with the specific inhibitor triacsin C, we examined whether acyl-CoA formation is required for efficient BMP synthesis. The inhibition of ACS drastically decreased BMP synthesis, indicating that acyl-CoA dependent acyltransferase are involved in this pathway. However, the reduced availability of acyl-CoA might also have side effects such as directing acyl-CoA to beta-oxidation or in the synthesis of other complex lipids. Furthermore, acyl-CoAs are regulatory factors affecting the activity of numerous enzymes[74]. To show a direct involvement of acyl-CoA dependent acyltransferase or PLD in BMP synthesis, it will be important to perform assays in cell lysates. Using cell lysates, it is possible to monitor BMP synthesis under controlled condition, allowing investigating the direct influence of acyl-CoA, pH, PLD and other factors on BMP biosynthesis.

The site of BMP synthesis is currently unknown. As BMP is mainly encountered in LE and lysosomes, it can be assumed that this is also the site of production using internalized lipids as precursors. Alternatively, it may be synthesized on the outer membrane of LE or in other compartments and then transported to LE. We asked if BMP synthesis happens in acidic (at pH 5.5) or neutral pH (pH 7.4), which would reflect late endosomal and cytosolic pH, respectively. To exclude that an acidic environment is required for BMP formation, we inhibited the V-ATPase of LE/lysosome with bafilomycin and monitored BMP increase after PG load. BMP synthesis remained unchanged even though the protonation of acidic organelles was inhibited. Hence, BMP synthesis does not require an acidic pH suggesting that BMP formation occurs at neutral pH on the surface of the LE/lysosome or other cytoplasmic compartments.

In order to get a better understanding of the conditions needed for BMP synthesis, it was necessary to establish an *in-vitro* assay system using cell lysates. We

investigated pH dependent formation of BMP by incubating COS7 cell lysates with PG ± oleoyl-CoA at pH 5.5 and 7.4, which resembled the pH of the LE/lysosome and cytoplasm. However, we could not observe BMP synthesis under the applied conditions. The addition of divalent ions moderately increased BMP formation indicating the contribution of Ca^{2+}/Mg^{2+} - dependent enzymes. However, this assay requires optimization of the reaction conditions.

A collaboration partner suggested that BMP can be synthesized extracellularly by so far uncharacterized enzymes secreted from macrophages (personal communication with Peter Greimel, RIKEN AICS · Brain Science Institute (BSI)). We used conditioned media of RAW macrophages to investigate its *in-vitro* capability to produce BMP. Notably, we observed a significant increase in PG-dependent BMP formation in conditioned media. This activity was reduced but not diminished by addition of EDTA suggesting that the responsible enzyme requires divalent ions for optimal catalytic activity. Thus, our observations demonstrate that BMP synthesis can also occur in the serum catalyzed by enzymes secreted from macrophages. This is in line with Heravi and White[27], who suggested that BMP synthesis can occur in different compartments and by different mechanisms.

The second aspect of this thesis focused on the implication of BMP in drug-induced phospholipidosis. BMP accumulates in many LSDs induced by mutations in specific genes or by drugs and BMP is also used as biomarker for LSD[53]. BMP accumulates secondary to traffic jam in acidic organelles and published data suggest that supplementation of BMP can improve the phenotype of NPC fibroblasts[37]. Currently it is unclear whether BMP is also protective against drug-induced cytotoxicity. Thus, we hypothesized that the increase of intracellular BMP is a protective cellular response against CADs. Notably, PG supplementation clearly reduced LDH release and SYTOX green staining demonstrating protective effects against amiodarone. From these experiments it was unclear whether the protective effects derive from PG or BMP. Since published data suggest that PG 16:0 cannot be used for BMP synthesis[65], we performed a control experiment using this lipid. In comparison to PG 18:1, PG 16:0 barely increased BMP formation and did not mediate protective effects indicating that efficient BMP synthesis is responsible for the protective effects.

The mechanisms behind the protective effects of BMP are currently unclear. Considering that BMP facilitates lipid sorting, we assume that it also facilitates the cellular sorting of CADs like amiodarone. It may improve secretion of CADs or improve the storage capacity of acidic organelles for such compounds. Accordingly, it will be necessary to perform additional experiments on secretion and storage of CADs. Furthermore, it will be important to investigate whether this protective effect is specific for amiodarone or also observable in the presence of other CADs.

The mode of action of CADs is not fully understood. Petersen et al.[59] showed that CADs increase LMP and cell death in tumor cells as they displace acid sphingomyelinase, hence increasing sphingomyelin content which destabilizes the lysosomal outer membrane. LMP can be determined by measuring cytosolic cathepsin levels, a protease that is trapped in lysosomes under physiological conditions. PG pretreatment showed no effect on cytosolic cathepsin activity, while CAD-treated cell displayed a 2-fold increase in activity. PG supplementation of CAD-treated cells reduced cathepsin activity to basal levels suggesting that PG counteracts LMP by stabilizing lysosomal membranes. Interestingly, induction of LMP has been shown in NPC cells. NPC is a metabolic disorder in which sphingomyelin accumulates in lysosomes caused by a defect in acid sphingomyelinase. Kirkegaard et al.[75] reported that heat shock protein 70 (Hsp70) associates with BMP, thereby facilitating the BMP binding and activity of ASM. Notably, cells from patients with NPA and NPB showed a decrease in lysosomal stability caused by reduced ASM activity, and this phenotype was effectively corrected by treatment with recombinant Hsp70. Our data suggest that lysosomal stability can be improved solely by increasing BMP. It remains to be investigated whether PG load also causes changes in the subcellular distribution of Hsp70.

In this thesis, we provide evidence that BMP synthesis can be induced in various cell lines by supplementation of PG. Our observations suggest that PLD1 and ACS are involved in the formation of BMP and that BMP is synthesized outside of acidic organelles. Furthermore, we observed that BMP synthesis can occur extracellularly by macrophage-derived enzymes. Finally, we show that PG-induced BMP formation reduces amiodarone-induced cytotoxicity by decreasing LMP. Currently, pathways regulating the synthesis of BMP remain elusive. Nonetheless, our data provide novel

insights into BMP formation and underline the importance of elucidating BMP biosynthesis for getting a better understanding of lysosomal function and dysfunction.

5. References

1. Body, D. R. & Gray, G. M. The isolation and characterisation of phosphatidylglycerol and a structural isomer from pig lung. *Chemistry and Physics of Lipids* **1**, 254–263 (1967).
2. Gruenberg, J. Lipids in endocytic membrane transport and sorting. *Curr. Opin. Cell Biol.* **15**, 382–388 (2003).
3. Gallala, H. D. & Sandhoff, K. Biological Function of the Cellular Lipid BMP—BMP as a Key Activator for Cholesterol Sorting and Membrane Digestion. *Neurochem Res* **36**, 1594–1600 (2011).
4. Hostetler, K. Y. Chapter 6 Polyglycerophospholipids: phosphatidylglycerol, diphosphatidylglycerol and bis (monoacylglycero) phosphate. in *New Comprehensive Biochemistry* (eds. Hawthorne, J. N. & Ansell, G. B.) **4**, 215–261 (Elsevier, 1982).
5. Brotherus, J., Renkonen, O., Herrmann, J. & Fischer, W. Novel stereoconfiguration in lyso-bis-phosphatidic acid of cultured BHK-cells. *Chemistry and Physics of Lipids* **13**, 178–182 (1974).
6. Mason, R. J., Stossel, T. P. & Vaughan, M. Lipids of alveolar macrophages, polymorphonuclear leukocytes, and their phagocytic vesicles. *J. Clin. Invest.* **51**, 2399–2407 (1972).
7. Wherrett, J. R. & Huterer, S. Bis-(monoacylglyceryl)-phosphate of rat and human liver: Fatty acid composition and NMR spectroscopy. *Lipids* **8**, 531–533 (1973).
8. Bouvier, J. *et al.* Selective decrease of bis(monoacylglycero)phosphate content in macrophages by high supplementation with docosahexaenoic acid. *J. Lipid Res.* **50**, 243–255 (2009).
9. Besson, N. *et al.* Selective incorporation of docosahexaenoic acid into lysobisphosphatidic acid in cultured THP-1 macrophages. *Lipids* **41**, 189–196 (2006).
10. Akgoc, Z., Iosim, S. & Seyfried, T. N. Bis(monoacylglycero)phosphate as a Macrophage Enriched Phospholipid. *Lipids* **50**, 907–912 (2015).
11. van der Goot, F. G. & Gruenberg, J. Intra-endosomal membrane traffic. *Trends Cell Biol.* **16**, 514–521 (2006).
12. Pryor, P. R. & Luzio, J. P. Delivery of endocytosed membrane proteins to the lysosome. *Biochim. Biophys. Acta* **1793**, 615–624 (2009).
13. Matsuo, H. *et al.* Role of LBPA and Alix in multivesicular liposome formation and endosome organization. *Science* **303**, 531–534 (2004).
14. Stoorvogel, W., Kleijmeer, M. J., Geuze, H. J. & Raposo, G. The biogenesis and functions of exosomes. *Traffic* **3**, 321–330 (2002).
15. Falguières, T., Luyet, P.-P. & Gruenberg, J. Molecular assemblies and membrane domains in multivesicular endosome dynamics. *Exp. Cell Res.* **315**, 1567–1573 (2009).
16. Schulze, H., Kolter, T. & Sandhoff, K. Principles of lysosomal membrane degradation: Cellular topology and biochemistry of lysosomal lipid degradation. *Biochim. Biophys. Acta* **1793**, 674–683 (2009).

17. Hullin-Matsuda, F., Luquain-Costaz, C., Bouvier, J. & Delton-Vandenbroucke, I. Bis(monoacylglycero)phosphate, a peculiar phospholipid to control the fate of cholesterol: Implications in pathology. *Prostaglandins, Leukotrienes and Essential Fatty Acids* **81**, 313–324 (2009).
18. Kobayashi, T. *et al.* Late endosomal membranes rich in lysobisphosphatidic acid regulate cholesterol transport. *Nat. Cell Biol.* **1**, 113–118 (1999).
19. Kobayashi, T. *et al.* A lipid associated with the antiphospholipid syndrome regulates endosome structure and function. *Nature* **392**, 193–197 (1998).
20. Sobo, K., Chevallier, J., Parton, R. G., Gruenberg, J. & van der Goot, F. G. Diversity of raft-like domains in late endosomes. *PLoS ONE* **2**, e391 (2007).
21. Kolter, T. & Sandhoff, K. Principles of lysosomal membrane digestion: stimulation of sphingolipid degradation by sphingolipid activator proteins and anionic lysosomal lipids. *Annu. Rev. Cell Dev. Biol.* **21**, 81–103 (2005).
22. Kolter, T. & Sandhoff, K. Sphingolipid metabolism diseases. *Biochimica et Biophysica Acta (BBA) - Biomembranes* **1758**, 2057–2079 (2006).
23. Kolter, T. & Sandhoff, K. Lysosomal degradation of membrane lipids. *FEBS Letters* **584**, 1700–1712 (2010).
24. Harder, A., Dodt, G. & Debuch, H. Amphiphilic cationic drugs and phospholipids influence the activities of beta-galactosidase and beta-glucosidase from liver lysosomal fraction of untreated rats. *Biol. Chem. Hoppe-Seyler* **366**, 189–193 (1985).
25. Makino, A. *et al.* D-threo-1-phenyl-2-decanoylamino-3-morpholino-1-propanol alters cellular cholesterol homeostasis by modulating the endosome lipid domains. *Biochemistry* **45**, 4530–4541 (2006).
26. Thornburg, T., Miller, C., Thuren, T., King, L. & Waite, M. Glycerol reorientation during the conversion of phosphatidylglycerol to bis(monoacylglycerol)phosphate in macrophage-like RAW 264.7 cells. *J. Biol. Chem.* **266**, 6834–6840 (1991).
27. Heravi, J. & Waite, M. Transacylase formation of bis(monoacylglycerol)phosphate. *Biochim. Biophys. Acta* **1437**, 277–286 (1999).
28. van Blitterswijk, W. J. & Hilkmann, H. Rapid attenuation of receptor-induced diacylglycerol and phosphatidic acid by phospholipase D-mediated transphosphatidylation: formation of bisphosphatidic acid. *EMBO J.* **12**, 2655–2662 (1993).
29. Pribasnig, M. A. *et al.* α/β Hydrolase Domain-containing 6 (ABHD6) Degrades the Late Endosomal/Lysosomal Lipid Bis(monoacylglycero)phosphate. *J. Biol. Chem.* **290**, 29869–29881 (2015).
30. Ito, M., Tchoua, U., Okamoto, M. & Tojo, H. Purification and Properties of a Phospholipase A_2 /Lipase Preferring Phosphatidic Acid, Bis(monoacylglycerol) Phosphate, and Monoacylglycerol from Rat Testis. *Journal of Biological Chemistry* **277**, 43674–43681 (2002).

31. Record, M. *et al.* Bis (monoacylglycero) phosphate interfacial properties and lipolysis by pancreatic lipase-related protein 2, an enzyme present in THP-1 human monocytes. *Biochimica et Biophysica Acta (BBA) - Molecular and Cell Biology of Lipids* **1811**, 419–430 (2011).
32. Blankman, J. L., Long, J. Z., Trauger, S. A., Siuzdak, G. & Cravatt, B. F. ABHD12 controls brain lysophosphatidylserine pathways that are deregulated in a murine model of the neurodegenerative disease PHARC. *Proceedings of the National Academy of Sciences* **110**, 1500–1505 (2013).
33. Sleat, D. E. *et al.* Mass spectrometry-based protein profiling to determine the cause of lysosomal storage diseases of unknown etiology. *Mol. Cell Proteomics* **8**, 1708–1718 (2009).
34. Rao, B. G. & Spence, M. W. Niemann-Pick disease type D: lipid analyses and studies on sphingomyelinases. *Ann. Neurol.* **1**, 385–392 (1977).
35. Rouser, G., Kritchevsky, G., Knudson, A. G. & Simon, G. Accumulation of a glycerolphospholipid in classical niemann-pick disease. *Lipids* **3**, 287–290 (1968).
36. Meikle, P. J. *et al.* Effect of lysosomal storage on bis(monoacylglycero)phosphate. *Biochem. J.* **411**, 71–78 (2008).
37. Jochum, A., Li, R., Newton, S., McCauliff, L. & Storch, J. The Unique Relationship between Niemann Pick Type C2 (NPC2) Protein and Lysobisphosphatidic Acid (LBPA). *The FASEB Journal* **30**, 658.2-658.2 (2016).
38. Vance, J. E. Lipid imbalance in the neurological disorder, Niemann-Pick C disease. *FEBS Lett.* **580**, 5518–5524 (2006).
39. Chapel, A. *et al.* An extended proteome map of the lysosomal membrane reveals novel potential transporters. *Mol. Cell Proteomics* **12**, 1572–1588 (2013).
40. Palmieri, M. *et al.* Characterization of the CLEAR network reveals an integrated control of cellular clearance pathways. *Hum. Mol. Genet.* **20**, 3852–3866 (2011).
41. Di Fruscio, G. *et al.* Lysoplex: An efficient toolkit to detect DNA sequence variations in the autophagy-lysosomal pathway. *Autophagy* **11**, 928–938 (2015).
42. Platt, F. M., d'Azzo, A., Davidson, B. L., Neufeld, E. F. & Tifft, C. J. Lysosomal storage diseases. *Nat Rev Dis Primers* **4**, 27 (2018).
43. Schröder, B. *et al.* Integral and associated lysosomal membrane proteins. *Traffic* **8**, 1676–1686 (2007).
44. Szklarczyk, D. *et al.* STRING v10: protein-protein interaction networks, integrated over the tree of life. *Nucleic Acids Res.* **43**, D447-452 (2015).
45. Late endosomal membranes rich in lysobisphosphatidic acid regulate cholesterol transport. - PubMed - NCBI. Available at: https://www.ncbi.nlm.nih.gov/pubmed/10559883. (Accessed: 13th November 2018)
46. Kahma, K., Brotherus, J., Haltia, M. & Renkonen, O. Low and moderate concentrations of lysobisphosphatidic acid in brain and liver of patients affected by some storage diseases. *Lipids* **11**, 539–544 (1976).

47. Harder, A., Widjaja, F. & Debuch, H. Studies on lipids from liver and spleen of a child (O.L.) with Niemann-Pick's disease type C. *J. Clin. Chem. Clin. Biochem.* **22**, 199–201 (1984).
48. Käkelä, R., Somerharju, P. & Tyynelä, J. Analysis of phospholipid molecular species in brains from patients with infantile and juvenile neuronal-ceroid lipofuscinosis using liquid chromatography-electrospray ionization mass spectrometry. *J. Neurochem.* **84**, 1051–1065 (2003).
49. Brotherus, J., Niinioja, T., Sandelin, K. & Renkonen, O. Experimentally caused proliferation of lysosomes in cultured BHK cells involving an increase of biphosphatidic acids and triglycerides. *J. Lipid Res.* **18**, 379–388 (1977).
50. Accumulation of a glycerolphospholipid in classical niemann-pick disease - Rouser - 1968 - Lipids - Wiley Online Library. Available at: https://onlinelibrary.wiley.com/doi/abs/10.1007/BF02531203. (Accessed: 13th November 2018)
51. Reasor, M. J. *et al.* Comparative evaluation of amiodarone-induced phospholipidosis and drug accumulation in Fischer-344 and Sprague-Dawley rats. *Toxicology* **106**, 139–147 (1996).
52. Muehlbacher, M., Tripal, P., Roas, F. & Kornhuber, J. Identification of Drugs Inducing Phospholipidosis by Novel in vitro Data. *ChemMedChem* **7**, 1925–1934 (2012).
53. Liu, N., Tengstrand, E. A., Chourb, L. & Hsieh, F. Y. Di-22:6-bis(monoacylglycerol)phosphate: A clinical biomarker of drug-induced phospholipidosis for drug development and safety assessment. *Toxicol. Appl. Pharmacol.* **279**, 467–476 (2014).
54. Pubchem. Amiodarone. Available at: https://pubchem.ncbi.nlm.nih.gov/compound/2157. (Accessed: 17th December 2018)
55. Amiodarone Side Effects in Detail. *Drugs.com* Available at: https://www.drugs.com/sfx/amiodarone-side-effects.html. (Accessed: 17th December 2018)
56. Flaharty, K. K., Chase, S. L., Yaghsezian, H. M. & Rubin, R. Hepatotoxicity associated with amiodarone therapy. *Pharmacotherapy* **9**, 39–44 (1989).
57. Hostetler, K. Y. Molecular studies of the induction of cellular phospholipidosis by cationic amphiphilic drugs. *Fed. Proc.* **43**, 2582–2585 (1984).
58. Pappu, A. & Hostetler, K. Y. Effect of cationic amphiphilic drugs on the hydrolysis of acidic and neutral phospholipids by liver lysosomal phospholipase A. *Biochem. Pharmacol.* **33**, 1639–1644 (1984).
59. Petersen, N. H. T. *et al.* Transformation-Associated Changes in Sphingolipid Metabolism Sensitize Cells to Lysosomal Cell Death Induced by Inhibitors of Acid Sphingomyelinase. *Cancer Cell* **24**, 379–393 (2013).
60. Boya, P. & Kroemer, G. Lysosomal membrane permeabilization in cell death. *Oncogene* **27**, 6434–6451 (2008).

61. Serrano-Puebla, A. & Boya, P. Lysosomal membrane permeabilization in cell death: new evidence and implications for health and disease: Lysosomal membrane permeabilization and neurodegeneration. *Annals of the New York Academy of Sciences* **1371**, 30–44 (2016).
62. Terman, A., Kurz, T., Gustafsson, B. & Brunk, U. Lysosomal labilization. *IUBMB Life (International Union of Biochemistry and Molecular Biology: Life)* **58**, 531–539 (2006).
63. Gómez-Sintes, R., Ledesma, M. D. & Boya, P. Lysosomal cell death mechanisms in aging. *Ageing Research Reviews* **32**, 150–168 (2016).
64. Folch, J., Lees, M. & Sloane Stanley, G. H. A simple method for the isolation and purification of total lipides from animal tissues. *J. Biol. Chem.* **226**, 497–509 (1957).
65. Luquain-Costaz, C. *et al.* Bis(Monoacylglycero)Phosphate Accumulation in Macrophages Induces Intracellular Cholesterol Redistribution, Attenuates Liver-X Receptor/ATP-Binding Cassette Transporter A1/ATP-Binding Cassette Transporter G1 Pathway, and Impairs Cholesterol Efflux. *Arteriosclerosis, Thrombosis, and Vascular Biology* **33**, 1803–1811 (2013).
66. Kobayashi, T. *et al.* Late endosomal membranes rich in lysobisphosphatidic acid regulate cholesterol transport. *Nat. Cell Biol.* **1**, 113–118 (1999).
67. Hullin-Matsuda, F. *et al.* De novo biosynthesis of the late endosome lipid, bis(monoacylglycero)phosphate. *J. Lipid Res.* **48**, 1997–2008 (2007).
68. Bae, E.-J. *et al.* Phospholipase D1 regulates autophagic flux and clearance of α-synuclein aggregates. *Cell Death Differ* **21**, 1132–1141 (2014).
69. Zhang, Y. & Frohman, M. A. Cellular and Physiological Roles for Phospholipase D1 in Cancer. *J Biol Chem* **289**, 22567–22574 (2014).
70. Ahn, B.-H. *et al.* Transmodulation between Phospholipase D and c-Src Enhances Cell Proliferation. *Molecular and Cellular Biology* **23**, 3103–3115 (2003).
71. Du, G., Huang, P., Liang, B. T. & Frohman, M. A. Phospholipase D2 Localizes to the Plasma Membrane and Regulates Angiotensin II Receptor Endocytosis. *Mol Biol Cell* **15**, 1024–1030 (2004).
72. Ha, S. H. *et al.* PLD2 forms a functional complex with mTOR/raptor to transduce mitogenic signals. *Cellular Signalling* **18**, 2283–2291 (2006).
73. Zheng, X., Ray, S. & Bollag, W. B. Modulation of phospholipase D-mediated phosphatidylglycerol formation by differentiating agents in primary mouse epidermal keratinocytes. *Biochimica et Biophysica Acta (BBA) - Molecular Cell Research* **1643**, 25–36 (2003).
74. Knudsen, J., Neergaard, T. B. F., Gaigg, B., Jensen, M. V. & Hansen, J. K. Role of Acyl-CoA Binding Protein in Acyl-CoA Metabolism and Acyl-CoA–Mediated Cell Signaling. *J Nutr* **130**, 294S-298S (2000).
75. Kirkegaard, T. *et al.* Hsp70 stabilizes lysosomes and reverts Niemann-Pick disease-associated lysosomal pathology. *Nature* **463**, 549–553 (2010).